

This discussion paper is/has been under review for the journal Biogeosciences (BG).
Please refer to the corresponding final paper in BG if available.

Seasonal evolution of net and regenerated silica production around a natural Fe-fertilized area in the Southern Ocean estimated from Si isotopic approaches

I. Closset¹, M. Lasbleiz², K. Leblanc², B. Quéguiner², A.-J. Cavagna³,
M. Elskens³, J. Navez⁴, and D. Cardinal^{1,4}

¹Sorbonne Universités (UPMC, Univ Paris 06)-CNRS-IRD-MNHN, LOCEAN Laboratory, 4 place Jussieu, 75005 Paris, France

²Aix Marseille Université CNRS, Université de Toulon, IRD, MIO UM 110, 13288, Marseille, France

³Earth and System Sciences & Analytical and Environmental Chemistry, Vrije Universiteit Brussel, Pleinlaan 2, 1050 Brussels, Belgium

⁴Department of Earth Sciences, Royal Museum for Central Africa, Leuvensesteenweg 13, 3080 Tervuren, Belgium

BGD

11, 6329–6381, 2014

Seasonal evolution of net and regenerated silica production

I. Closset et al.

Title Page

Abstract

Introduction

Conclusions

References

Tables

Figures

◀

▶

◀

▶

Back

Close

Full Screen / Esc

Printer-friendly Version

Interactive Discussion



Received: 20 March 2014 – Accepted: 26 March 2014 – Published: 5 May 2014

Correspondence to: I. Closset (ivia.closset@locean-ipsl.upmc.fr)

Published by Copernicus Publications on behalf of the European Geosciences Union.

BGD

11, 6329–6381, 2014

**Seasonal evolution of
net and regenerated
silica production**

I. Closset et al.

Title Page

Abstract

Introduction

Conclusions

References

Tables

Figures



Back

Close

Full Screen / Esc

Printer-friendly Version

Interactive Discussion



Abstract

A massive diatom-bloom is observed each year in the surface waters of the naturally Fe fertilized Kerguelen Plateau (Southern Ocean). We measured biogenic silica production and dissolution fluxes in the mixed layer in the vicinity of the Kerguelen Plateau during austral spring 2011 (KEOPS-2 cruise). We compare results from a High-Nutrient Low-Chlorophyll reference station and stations with different degrees of iron enrichment and bloom conditions. Above the Plateau biogenic silica production fluxes are among the highest reported so far in the Southern Ocean (up to $47.9 \text{ mmol m}^{-2} \text{ d}^{-1}$). Although significant ($10.2 \text{ mmol m}^{-2} \text{ d}^{-1}$ in average), silica dissolution rates were generally much lower than production rates. Uptake ratios (Si:C and Si:N) confirm that diatoms strongly dominate the primary production in this area. At the bloom onset, decreasing dissolution to production ratios ($D:P$) indicate that the remineralization of silica could sustained most of the low silicon uptake and that the system progressively shifts toward a silica production regime which must be mainly supported by new source of silicic acid. Moreover, by comparing results from the two KEOPS-expeditions (spring 2011 and summer 2005), we suggest that there is a seasonal evolution on the processes decoupling Si and N cycles in the area. Indeed, the consumption of H_4SiO_4 standing stocks occurs only during the growing stage of the bloom when strong net silica production is observed, contributing to a higher H_4SiO_4 depletion relative to NO_3^- . Then, the decoupling between H_4SiO_4 and NO_3^- is mainly controlled by the more efficient nitrogen recycling relative to Si. Gross-Si:N uptake ratios were higher in the Fe-rich regions compared to the HNLC area, likely due to different diatoms communities. This suggests that the diatom responses to natural Fe fertilization are more complex than previously thought, and that natural iron fertilization over long time scales does not necessarily decrease Si:N uptake ratios as suggested by the Silicic Acid Leakage Hypothesis. Finally, we propose the first seasonal estimate of Si-biogeochemical budget above the Kerguelen Plateau based on direct measurements. This study points out that naturally iron fertilized areas of the Southern Ocean could sustain very high regimes

BGD

11, 6329–6381, 2014

Seasonal evolution of net and regenerated silica production

I. Closset et al.

Title Page

Abstract

Introduction

Conclusions

References

Tables

Figures

◀

▶

◀

▶

Back

Close

Full Screen / Esc

Printer-friendly Version

Interactive Discussion



of biogenic silica production, similar to those observed in highly productive upwelling systems.

1 Introduction

Covering 20% of the World Ocean, the Southern Ocean is considered as a crucial component of the climate system since it represents a net sink for atmospheric CO₂ (Takahashi et al., 2009). It also plays a key role in the global silicon (Si) biogeochemical cycle because diatoms, a siliceous phytoplankton group, are one of the major primary producers in this area (Buesseler et al., 2001; Quéguiner and Brzezinski, 2002; Tréguer and De la Rocha, 2013). As their cell wall is composed of biogenic silica (opal, hereafter referred to as BSi), diatoms take up dissolved silicon (hereafter referred to as DSi) in the form of silicic acid (H₄SiO₄), to produce their siliceous frustules. At global scale, 56% of this gross production is estimated to be directly recycled in the upper 100 m (Tréguer and De La Rocha, 2013) due to the combined effects of both physico-chemical and biological processes (Kamatani, 1982; Bidle and Azam, 1999; Ragueneau et al., 2000). Only the material escaping dissolution is exported toward the deep ocean and eventually buried in sediments. Consequently, the marine Si biogeochemical cycle is dominated by biogenic silica production and dissolution in the surface mixed layer, and one atom of Si undergoes a cycle of biological uptake by diatom and subsequent dissolution about 25 times before being removed to the seabed (Tréguer and De La Rocha, 2013). Thus, it is essential to estimate the balance between silica production and dissolution in the euphotic zone which is best illustrated by the integrated dissolution to production rate ratio ($\int D : \int P$; Brzezinski et al., 2003) or by integrated net production rate ($\int \rho_{\text{Net}}$ = production minus dissolution). Globally, the $\int D : \int P$ values present an annual mean of 0.56 (Tréguer and De La Rocha, 2013) and range from < 0.1 to > 1, with low $D : P$ values associated to diatom bloom events, and $D : P$ values exceeding 0.5 occurring during non-bloom periods (Brzezinski et al., 2001). However, the number of $D : P$ estimates, due to a small number of Si uptake measurements and an even lower

Seasonal evolution of net and regenerated silica production

I. Closset et al.

Title Page

Abstract

Introduction

Conclusions

References

Tables

Figures



Back

Close

Full Screen / Esc

Printer-friendly Version

Interactive Discussion



number of Si dissolution measurements, is insufficient compared to the high variability observed regionally and seasonally in the ocean which implies high uncertainty in the global $D : P$ estimate and overall on the marine silicon budget.

Diatoms are ecologically widespread and dominate the primary production in the Antarctic Circumpolar Current (ACC), especially south of the Polar Front (PF), where their productivity accounts for 1/3 of the global marine silica production (Pondaven et al., 2000; Buesseler et al., 2001). Consequently, this part of the Southern Ocean represents a key study area to improve our understanding of the global biogeochemical cycles of both carbon and silicon. Biological processes occurring in the Southern Ocean have indeed a significant impact on global biogeochemistry. For example, the large H_4SiO_4 utilization by diatoms in the ACC, combined to the global overturning circulation would determine the functioning of the biological pump of low latitude areas by inducing a strong silicic acid limitation (Sarmiento et al., 2004). In the Southern Ocean, a much larger depletion of silicic acid than nitrate in surface waters occurs (Trull et al., 2001), which results from the action of a silicon pump, i.e. the preferential export of BSi compared to particulate organic nitrogen (PON; Dugdale et al., 1995). This area is also the largest High Nutrient Low Chlorophyll (HNLC) zone of the global ocean where dissolved iron limitation plays a fundamental role in regulating the primary production and the carbon cycle (De Baar et al., 2005; Boyd et al., 2007; Tagliabue et al., 2012). Indeed, phytoplankton community structure and nutrient cycling could be largely controlled by Fe availability, with highest growth rates located close to iron sources such as continental margins, island systems and frontal regions (Blain et al., 2007; Tagliabue et al., 2012).

In this context, the Kerguelen Ocean and Plateau compared Study (KEOPS) program, consisting of two expeditions (late summer 2005 and early spring 2011), was conducted to investigate a naturally iron-fertilized area located in the Indian sector of the Southern Ocean, where the iron availability could potentially favor the carbon and silicon biological pumps (Fig. 1; Blain et al., 2007). Two massive and complex blooms, which are clearly constrained by the local bathymetry, are observed annu-

BGD

11, 6329–6381, 2014

Seasonal evolution of net and regenerated silica production

I. Closset et al.

Title Page

Abstract

Introduction

Conclusions

References

Tables

Figures

◀

▶

◀

▶

Back

Close

Full Screen / Esc

Printer-friendly Version

Interactive Discussion



ally over the Kerguelen Plateau and contrasts with the HNLC character of surrounding waters (Pollard et al., 2002; Mongin et al., 2008). The first KEOPS expedition (KEOPS-1, January–February 2005) has highlighted the impact of natural iron fertilization on primary production and nutrient cycling, as well as the advantages to study natural laboratories in the context of such ocean fertilization (Blain et al., 2008). The general purpose of KEOPS-2 (October–November 2011) was to improve our knowledge about the processes responsible for this iron fertilization and its impact on the seasonal variations of the mechanisms controlling the primary production and carbon export. While the KEOPS-1 cruise was mainly directed towards the study of the bloom in the South-East area of the Plateau, KEOPS-2 focused mainly on the bloom located North-East of the Kerguelen Islands above the Kerguelen abyssal plain.

In this paper, we investigate the spatial and seasonal variability of silica production and dissolution in the surface waters of the Kerguelen area. The specific objectives are the following:

- Compare the Si cycle dynamics in contrasting productive environments such as the southeastern Kerguelen Plateau bloom, the northeastern Kerguelen bloom in a stationary meander southward the PF and the warmer waters located north of this front, relative to the upstream HNLC area south-west of Kerguelen Islands, and identify controlling processes.
- Determine and quantify the seasonal evolution of processes which drive the Si biogeochemical budget in the upper layer of the Kerguelen Plateau, using the ^{30}Si stable isotope method (Nelson and Goering, 1977a; Fripiat et al., 2009) applied during KEOPS-2 and other techniques of mass and isotopic balance used during KEOPS-1 (^{32}Si radiogenic tracer incubations; Mosseri et al., 2008 and natural silicon isotopic composition, $\delta^{30}\text{Si}$; Fripiat et al., 2011a), in order to fully characterize the silicon cycle above the Kerguelen Plateau.
- Finally, compare our dataset with previous results in other productive regions of the global ocean and discuss the different types of diatom dominated regimes.

Seasonal evolution of net and regenerated silica production

I. Closset et al.

Title Page

Abstract

Introduction

Conclusions

References

Tables

Figures



Back

Close

Full Screen / Esc

Printer-friendly Version

Interactive Discussion



2 Material and methods

2.1 KEOPS-2 sampling campaign

The KEOPS-2 cruise was conducted in the Indian sector of the Southern Ocean during the austral spring 2011 (from 10 October to 20 November) on board the R/V Marion Dufresne (TAAF/IPEV) and was focused on the iron-fertilized blooms observed around the Kerguelen Plateau region. This plateau is a large area of relatively shallow seafloor that acts as a barrier to the circumpolar flow of the ACC, forcing a large part of the current to pass north of the plateau. The remaining flow passes south of the Kerguelen Islands and forms the jet of the PF, which exhibits strong meandering and eddy activity (Park et al., 2008, 1998; Roquet et al., 2009). As a consequence, the shallow region located south of Kerguelen Island represents a zone of weak north-eastward circulation (Park et al., 2008; Roquet et al., 2009) and bears a capacity of high chlorophyll *a* and BSi accumulation during phytoplankton blooms (Blain et al., 2001; Mosseri et al., 2008; Mongin et al., 2008). Over the plateau, enhanced vertical mixing associated to internal waves interact with the local bathymetry (Park et al., 2008) and supply iron and macronutrients from depth to surface waters, enabling to fuel phytoplankton bloom (Fripiat et al., 2011a; Blain et al., 2007).

The cruise consisted in 2 transects oriented south to north and west to east aimed at documenting the spatial extension of the bloom and its coastal-offshore gradient; and 8 long-term stations devoted to process studies with incubation experiments (Fig. 1). Except for one station (E4E) where we were not able to measure silica dissolution, Si fluxes were investigated in all these process-stations which characteristics are presented in Table 1:

- A HNLC reference station (R) located in deep waters south-west of Kerguelen Islands.
- The Kerguelen Plateau bloom reference station of KEOPS-1 (A3).

BGD

11, 6329–6381, 2014

Seasonal evolution of net and regenerated silica production

I. Closset et al.

Title Page

Abstract

Introduction

Conclusions

References

Tables

Figures

◀

▶

◀

▶

Back

Close

Full Screen / Esc

Printer-friendly Version

Interactive Discussion



- A productive open ocean station (F) influenced by warmer Sub-Antarctic Surface Water, located north of the Polar Front.
- A productive station (E4W) located in the plume of chlorophyll observed downstream of the plateau and close to the jet induced by the PF.
- 4 stations (E1 to E5) constituting a pseudo-lagrangian survey located in a complex recirculation zone in a stationary meander of the Polar front characterized by strong mesoscale activity (Zhou et al., 2014).

2.2 Sample collection, spike and incubation conditions

The isotopic dilution technique adapted by Fripiat et al. (2009) from Corvaisier et al. (2005) aims at simultaneously determining the rates of Si uptake (i.e. silica production) and of biogenic silica dissolution in the same seawater sample. After spiking with a solution enriched in ^{30}Si followed by incubation of the samples, the production rate is estimated from the change in isotopic composition of the particulate phase (increase in ^{30}Si). Similarly, the isotopic dilution (increase in ^{28}Si) in the ^{30}Si enriched seawater, due to the dissolution of naturally ^{28}Si enriched BSi initially present, is used to estimate the dissolution rate.

Production and dissolution rates were determined at 7 and 5 depths respectively, corresponding to different levels of Photosynthetically Active Radiation (PAR), from 75 % to 0.1 % of surface irradiance. Seawater was collected at defined depths in the euphotic layer using Niskin bottles mounted on a CTD-rosette. For each depth, 5 L of seawater were sampled. 1 L was subsampled to obtain a natural silicon isotopic standard (i.e. not spiked with ^{30}Si) to be processed along with the samples to correct for the matrix effect and mass bias during isotopic analysis (Fripiat et al., 2009). These unspiked samples were immediately filtered on 0.8 μm Nuclepore polycarbonate membranes to separate biogenic silica from silicic acid. The membrane was dried at 50 °C overnight and the filtrate was directly preconcentrated (see Sect. 2.3) and stored at room temperature in the dark.

Seasonal evolution of net and regenerated silica production

I. Closset et al.

Title Page

Abstract

Introduction

Conclusions

References

Tables

Figures



Back

Close

Full Screen / Esc

Printer-friendly Version

Interactive Discussion



The remaining seawater volume was subsampled in 2 L aliquots spiked with $\text{H}_4^{30}\text{SiO}_4$ -enriched solution (99 % ^{30}Si). Aliquots devoted to production measurements were spiked with a spike contribution representing usually less than 10 % of natural concentrations to minimize the perturbation of the natural DSi contents (Nelson and Goering, 1977a). In order to improve the detection limit of the method for dissolution, a second 2 L aliquot was spiked by adding ^{30}Si in the same amount as natural DSi (i.e. DSi spike addition at 100 % of the initial DSi). This provided sufficient sensitivity for the isotopic measurements of dissolution (see Sect. 3.1).

Immediately after spike addition and gentle mixing, 1 L was filtered following the same procedure than for the unspiked standard, to determine the initial conditions (t_0). The second half of the sample was poured into polycarbonate incubation-bottles and incubated under light conditions simulating those prevailing in situ for 24 h (10 % spiked samples) and for 48 h (100 % spiked samples). Deck-incubators were fitted with blue plastic optical filters to simulate the light attenuation of the corresponding sampling depths, and temperature was regulated by circulating surface seawater. At the end of the incubation period, samples were filtered and treated as described above to characterize the final conditions of the incubation (t_{24} or t_{48}).

2.3 Sample preparation and isotopic measurements

Preconcentration of H_4SiO_4 was applied on-board to increase the samples Si : salinity ratio, because the maximum salinity of the solution that can be introduced in the mass spectrometer is about 2 % (Fripiat et al., 2009). This step was achieved using a protocol adapted from the MAGIC method (Karl and Tien, 1992; Reynolds et al., 2006). The H_4SiO_4 was scavenged by the brucite precipitate ($\text{Mg}(\text{OH})_2$) obtained by adding 1 mL of 14 N NaOH to the 1 L of seawater sample and strong stirring. The precipitate was recovered by decantation and centrifugation, and was then dissolved in 3 mL of 3 N HCl.

In the shore based laboratory, polycarbonate membranes (t_0 , t_{24} and t_{48}) were digested in one step using a protocol adapted from Ragueneau et al. (2005) with 4 mL of

BGD

11, 6329–6381, 2014

Seasonal evolution of net and regenerated silica production

I. Closset et al.

Title Page

Abstract

Introduction

Conclusions

References

Tables

Figures

◀

▶

◀

▶

Back

Close

Full Screen / Esc

Printer-friendly Version

Interactive Discussion



0.2 N NaOH during 40 min at 100 °C to hydrolyse BSi. Samples were then neutralized with 1 mL of 1 N HCl to stop the reaction.

An aliquot of the solutions obtained after preconcentration and digestion was used to determine colorimetrically the DSi and BSi concentrations, following the method of Strickland and Parsons (1972). The remaining sample was diluted to 100 ppb Si in a 2% HNO₃ solution to determine the initial and final Si isotopic composition of the dissolved and particulate phases using a Element 2 (Thermo-Fischer) HR-SF-ICP-MS (High Resolution – Sector Field – Inductively Coupled Plasma – Mass Spectrometer) with the same configuration used by Fripiat et al. (2009).

3 Results

3.1 Accuracy of the model, detection limit and standard deviation

To estimate the production and dissolution of biogenic silica (ρ_{Si} and ρ_{Diss} , respectively), two different models are available: the linear one-compartmental model described by Nelson and Goering (1977a, b) and the non-linear two-compartmental model described in Elskens et al. (2007) and de Brauwere et al. (2005).

The mass and isotopic balance is not taken into account in the one compartmental model i.e. Si fluxes are calculated separately using the following equations:

$$\rho_{\text{Si}} = [\text{BSi}] \times \frac{\text{æBSi}_t}{t \times \text{æDSi}_{t0}} \quad (1)$$

$$\rho_{\text{Diss}} = [\text{DSi}] \times \frac{\text{æDSi}_{t0} - \text{æDSi}_t}{t \times \text{æDSi}_{t0}} \quad (2)$$

where [BSi] and [DSi] are the dissolved silicon and biogenic silica concentrations (in $\mu\text{mol L}^{-1}$); æBSi and æDSi are the abundance in excess (measured minus natural abundances) of ³⁰Si in the particulate and dissolved phase respectively; the subscribes t_0 and t refer to the initial and final incubation values.

Seasonal evolution of net and regenerated silica production

I. Closset et al.

Title Page

Abstract

Introduction

Conclusions

References

Tables

Figures



Back

Close

Full Screen / Esc

Printer-friendly Version

Interactive Discussion



By contrast, the two-compartmental model takes into account both isotopic composition and concentration changes occurring during the incubation time. Lack of consideration of these changes could induce significant biases in the estimated fluxes (Elskens et al., 2007). In this model the fluxes are estimated by resolving a system of 4 equations given by:

$$[\text{DSi}]_t = [\text{DSi}]_{t_0} + (\rho\text{Diss} - \rho\text{Si}) \times t \quad (3)$$

$$[\text{BSi}]_t = [\text{BSi}]_{t_0} \times (\rho\text{Si} - \rho\text{Diss}) \times t \quad (4)$$

$$\alpha\text{DSi}_t = \alpha\text{DSi}_{t_0} \times \left(1 + \frac{\rho\text{Diss} - \rho\text{Si}}{[\text{DSi}]_{t_0}} \times t \right)^{\frac{\rho\text{Diss}}{\rho\text{Si} - \rho\text{Diss}}} \quad (5)$$

$$\alpha\text{BSi}_t = \frac{\alpha\text{DSi}_{t_0} \times [\text{DSi}]_{t_0}}{[\text{BSi}]_{t_0} + (\rho\text{Si} - \rho\text{Diss}) \times t} \times \left(1 - \left(1 + \frac{\rho\text{Diss} - \rho\text{Si}}{[\text{DSi}]_{t_0}} \times t \right)^{\frac{\rho\text{Si}}{\rho\text{Si} - \rho\text{Diss}}} \right) \quad (6)$$

The best solution is found numerically by optimizing parameter values (ρSi and ρDiss) and minimizing the cost function (weighted sum of squared differences between calculated and measured variables, $[\text{BSi}]$, $[\text{H}_4\text{SiO}_4]$, αBSi , αDSi) for the four equations simultaneously (Elskens et al., 2007; de Brauwere et al., 2005).

The relevance of these 2 models against a given data set has already been discussed by Fripiat et al. (2011b) and Elskens et al. (2007). Taking into account these considerations, and after testing the accuracy and the sensitivity of each model, we will use preferentially the non-linear 2 compartmental model to estimate the biogenic silica production and dissolution during KEOPS-2. Due to unexpected sampling problems on-board, we were not able to measure $[\text{DSi}]_t$. Thus, in addition to the biogenic silica production and dissolution rates, this variable was also estimated by the model (Eqs. 3–6). Under these conditions, we lose one degree of freedom but the system remains identifiable since there are 3 unknowns and 4 equations.

KEOPS-2 took place during the onset of the blooms, the biogenic silica production rates were quite high and far above the detection limit, except for 3 depths of the HNLC

Seasonal evolution of net and regenerated silica production

I. Closset et al.

Title Page

Abstract

Introduction

Conclusions

References

Tables

Figures



Back

Close

Full Screen / Esc

Printer-friendly Version

Interactive Discussion



reference station (R) and for the deepest value at each station (0.01 % PAR attenuation depth, 8 samples). However, since biogenic silica dissolution rates were expected to be low in early spring, it is essential to determine the limit of detection for the ^{30}Si isotopic dilution.

In most cases, final δDSi were significantly different from initial δDSi (paired T test, p value < 0.001). The detection limit for isotopic dilution was then estimated as being the lowest difference between initial and final ^{30}Si isotopic abundances ($\Delta\delta\text{DSi}$) measurable by the instrument. Every δDSi solutions have been analyzed in duplicates with a pooled standard deviation of 0.32 % ($n = 35$). In addition, we analyzed the same internal standard several times during every analytical session. The relative standard deviation (RSD) on δDSi of this in-house standard solution is 0.43 % ($n = 40$) and represents the long-term reproducibility of HR-SF-ICP-MS measurements. Therefore, each KEOPS-2 incubation with a $\Delta\delta\text{DSi}$ between t_0 and t_{48} higher than this RSD was considered to be significantly different from zero, and hence above the detection limit. This was the case for almost all the KEOPS-2 dataset (see e.g. Fig. 2), except for 7 values showing a change in ^{30}Si abundance below the detection limit. This included 4 samples from the HNLC reference station R where biological activity was extremely low.

Due to time and sampled water volume constraints, the sampling strategy adopted for KEOPS-2 gave the priority to highest vertical resolution instead of replicate incubations. Since only the analytical reproducibility was taken into account in the model, the standard deviations on Si uptake and dissolution rates were likely to be underestimated. Therefore we will use a theoretical relative precision for the whole incubation experiments of 10 %, as estimated for Si uptake rates by Fripiat et al. (2009).

3.2 Physical, chemical and biological parameters

The vertical structure of upper layer waters in the area was characteristic of the Antarctic Surface Water in the vicinity of the Polar Front (Park et al., 1998, 2008). The Winter Water (WW), identified by the minimum of temperature centered around 200 m, was

BGD

11, 6329–6381, 2014

Seasonal evolution of net and regenerated silica production

I. Closset et al.

Title Page

Abstract

Introduction

Conclusions

References

Tables

Figures

⏪

⏩

◀

▶

Back

Close

Full Screen / Esc

Printer-friendly Version

Interactive Discussion



capped by a homogeneous mixed layer (ML) induced by seasonal stratification. The boundary between the surface ML and the WW is usually marked by a strong seasonal pycnocline. However, at some stations, the stratification of the surface layer was relatively complex and showed two successive discontinuities evidenced by two different density gradients as indicated in Fig. 3.

During KEOPS-2, the surface ML depth, defined by the density difference of 0.02 from the surface (Park et al., 2014), showed a large variability between stations (Fig. 3). A strong and shallow stratification was measured north of the polar front, while wind events induced weak stratification and deep ML in the stations above the plateau and in the HNLC area. Stations in the recirculation zone (E1 to E5) supported a complex stratification due to their highly spatial and temporal dynamic and were characterized by 2 distinct density discontinuities.

All the stations located south of the Polar Front had quite homogeneous Chl *a*, BSi and DSi stocks from the surface to the deepest density discontinuity (below the so-called ML; Fig. 3). North of the Polar Front, these stocks were higher at the surface and decreased with depth (Fig. 3c). Stations A3 and E4W present similar BSi and DSi surface concentrations (Fig. 3e and g). At these 2 stations, DSi concentrations increase gradually while Chl *a* and BSi decrease drastically below the deepest density discontinuity. Station R contrasted from the latter stations by its low BSi, low Chl *a* content and relatively high DSi concentrations, confirming its HNLC character (Fig. 3a). During the lagrangian survey (stations E1, E3, E4E and E5), we observed a DSi depletion from ≈ 15 to $\approx 10 \mu\text{molL}^{-1}$ in surface waters, an increase of Chl *a* concentrations from < 1 to $> 1 \text{mgm}^{-3}$ and a doubling of the BSi content from ≈ 1.5 to $> 3 \mu\text{molL}^{-1}$ (Fig. 3b, d, f and h). Such temporal variations were mainly driven by diatom production as described below.

3.3 Biogenic silica production and dissolution rates

Silica production rates were quite homogeneously distributed in the euphotic layer with an exception for the station F located north of the Polar Front where it decreases pro-

Discussion Paper | Discussion Paper | Discussion Paper | Discussion Paper | Discussion Paper

BGD

11, 6329–6381, 2014

Seasonal evolution of net and regenerated silica production

I. Closset et al.

Title Page

Abstract

Introduction

Conclusions

References

Tables

Figures

⏪

⏩

◀

▶

Back

Close

Full Screen / Esc

Printer-friendly Version

Interactive Discussion



gressively with depth (Fig. 4a). Surface ρSi varied from $0.036 \pm 0.003 \mu\text{mol L}^{-1} \text{d}^{-1}$ (R in the HNLC area) to $1.28 \pm 0.12 \mu\text{mol L}^{-1} \text{d}^{-1}$ (A3, above the Plateau). All over the study area, Si uptake rates reached very low values at the base of the euphotic layer. Note that the same decreasing trend was also observed in primary production experiments performed in parallel (see e.g. Cavagna et al., 2014).

BSi dissolution rates were considerably lower than Si uptake rates except in the HNLC area (R) and at station E3 where ρSi was in the lower range of the KEOPS-2 dataset. Vertical profiles of ρDiss (Fig. 4b) were quite homogeneous from the surface to the base of the euphotic layer and did not increase at depth. This indicates that, the physical and biogeochemical processes affecting BSi dissolution did not vary significantly over the water column. This is also consistent with the low accumulation of biogenic silica observed at depth in spring (Lasbleiz et al., 2014) which contrasts with the occurrence of deep BSi maxima at the end of summer (Mosseri et al., 2008). Moreover, silica dissolution rates were not significantly different between bloom stations, and were comparable to those measured by Brzezinski et al. (2001) for the same season in the Pacific sector and by Beucher et al. (2004) and Fripiat et al. (2011b) for the end of summer in the Australian sector.

As silica production was close to zero below the euphotic layer, all the vertically integrated values presented in Table 2 were calculated from 100 % to 1 % of the surface PAR. The integrated Si uptake rates ($\int \rho\text{Si}$) varied from $3.09 \pm 0.01 \text{ mmol m}^{-2} \text{d}^{-1}$ (R, in the HNLC area) to $47.9 \pm 0.4 \text{ mmol m}^{-2} \text{d}^{-1}$ (A3, above the Plateau), and were among the highest reported so far in the Southern Ocean (see review in Fripiat, 2010). Integrated BSi dissolution rates ($\int \rho\text{Diss}$) were generally much lower than integrated production rates with values ranging from $3.79 \pm 0.03 \text{ mmol m}^{-2} \text{d}^{-1}$ north of the Polar Front (F) to $9.99 \pm 0.03 \text{ mmol m}^{-2} \text{d}^{-1}$ at E3. Because $\int \rho\text{Diss}$ did not vary over depth, or between stations, integrated dissolution estimates were correlated with the depth of the euphotic layer (Z_e), with higher values in stations with deeper Z_e , e.g. E1 and E3 ($R^2 = 0.83$, not shown).

Seasonal evolution of net and regenerated silica production

I. Closset et al.

[Title Page](#)[Abstract](#)[Introduction](#)[Conclusions](#)[References](#)[Tables](#)[Figures](#)[◀](#)[▶](#)[◀](#)[▶](#)[Back](#)[Close](#)[Full Screen / Esc](#)[Printer-friendly Version](#)[Interactive Discussion](#)

Net production rate of BSi in the euphotic layer ($\int \rho Si_{net}$) represents the difference between gross silica production and dissolution rates (Fig. 5) and could be associated to an uptake of “new- H_4SiO_4 ” i.e. that does not come from remineralisation processes within the ML. As for the net primary production, the net silica production could be defined as the part of the BSi that accumulates in the surface layer during the productive period, which would then be potentially available later for export to the mesopelagic layer (Brzezinski et al., 2001; Quéguiner, 2013). During the pseudo-lagrangian survey, net silica production was quite low during the first 2 visits (E1 and E3 with respectively 9.6 ± 0.1 and $0.5 \pm 0.1 \text{ mmol m}^{-2} \text{ d}^{-1}$) and reached the maximal value at the last visit (E5, $20.5 \pm 0.2 \text{ mmol m}^{-2} \text{ d}^{-1}$). The highest net production rate was observed above the Kerguelen Plateau (A3, $43.4 \pm 0.4 \text{ mmol m}^{-2} \text{ d}^{-1}$). In the HNLC area (Station R), silica dissolution was higher than silica production, leading to a negative $\int \rho Si_{net}$ ($-1.78 \pm 0.02 \text{ mmol m}^{-2} \text{ d}^{-1}$).

3.4 Specific rates of production and dissolution

The specific Si uptake rate (V_{Si}, d^{-1}) and dissolution rate (V_{Diss}, d^{-1}) give the fraction of the BSi pool produced or dissolved in one day as follows:

$$V_{Si} = \frac{\rho_{Si}}{[BSi]} \quad (7)$$

and

$$V_{Diss} = \frac{\rho_{Diss}}{[BSi]} \quad (8)$$

V_{Si} is mainly impacted by nutrient and/or light limitation (Claquin et al., 2002; Frank et al., 2000; Leynaert et al., 2004) and by the diatom community composition (Leynaert et al., 2004). During KEOPS-2, V_{Si} values (profiles not shown) presented the same decreasing trends with depth as Si uptake, which is consistent with an impact of

BGD

11, 6329–6381, 2014

Seasonal evolution of net and regenerated silica production

I. Closset et al.

Title Page

Abstract

Introduction

Conclusions

References

Tables

Figures

◀

▶

◀

▶

Back

Close

Full Screen / Esc

Printer-friendly Version

Interactive Discussion



light limitation on silica production. Globally, relatively high integrated specific Si-uptake rates ($\int VSi$) prevailed for KEOPS-2 (≈ 0.1 to $\approx 0.3 \text{ d}^{-1}$; Table 2). Such values are not different from those of nutrient-replete diatoms growing in the open ocean zone of the Southern Ocean (Brzezinski et al., 2001). By contrast, the HNLC area showed a $\int VSi$ value below 0.1 d^{-1} , suggesting non-optimal conditions for the growth of diatoms.

$\int VDiss$ varied around one order of magnitude during KEOPS-2 with low specific rates in productive stations (e.g. 0.03 d^{-1} above the Plateau), and higher values in the HNLC area (up to 0.15 d^{-1}). Interestingly, E3 showed unexpected high $\int VDiss$ (0.12 d^{-1} ; Table 2).

4 Discussion

4.1 Seasonality of the balance between silica production and dissolution

The $D:P$ ratios integrated between the surface and the 1% PAR attenuation depth ($\int D:\int P$; also summarized in Table 3) are presented in Fig. 5. At the HNLC reference station R, the $\int D:\int P$ value > 1 indicates that the integrated dissolution rate exceeds the measured integrated production rate (note that both fluxes were very low in the case of R). This situation leads to a net loss of biogenic silica by dissolution in the euphotic zone and suggests that a short development of diatoms could have occurred before our sampling. This observation is in accordance with the high barium excess measured between 200 and 400 m at R (Jacquet et al., 2014), indicating a high carbon mineralization activity in the mesopelagic zone which could be likely associated to a surface production event prior sampling. High $\int D:\int P$ values have already been measured occasionally in the Southern Ocean during the summer bloom (review in Tréguer and De La Rocha, 2013).

In the Kerguelen bloom area, $\int D:\int P$ ratios ranged from 0.09 (station A3) to 0.95 (station E3) and depended on the stage of the blooms. The $\int D:\int P$ ratios were relatively high at stations visited in the beginning of the cruise, indicating that a significant

BGD

11, 6329–6381, 2014

Seasonal evolution of net and regenerated silica production

I. Closset et al.

Title Page

Abstract

Introduction

Conclusions

References

Tables

Figures

◀

▶

◀

▶

Back

Close

Full Screen / Esc

Printer-friendly Version

Interactive Discussion



Seasonal evolution of net and regenerated silica production

I. Closset et al.

Title Page

Abstract

Introduction

Conclusions

References

Tables

Figures



Back

Close

Full Screen / Esc

Printer-friendly Version

Interactive Discussion



fraction of silica was recycled in the surface waters in early spring, and then decreased as the bloom took place. The highest $\int D : \int P$ ratio occurred at station E3. This station was characterized by a low BSi stock ($83.6 \text{ mmol Si m}^{-2}$), a low integrated BSi production rate ($10.5 \text{ mmol Si m}^{-2} \text{ d}^{-1}$ integrated over the euphotic layer; Table 2), a dissolution rate close to the mean for all stations, and high specific dissolution rate. This may evidence a higher relative proportion of detrital silica free of organic matter at this station which could be due to stronger bacterial and/or grazing activities inducing a top-down control on diatom growth. This observation is consistent with the higher abundance of fecal pellets measured in sediment trap samples at this station. Without considering E3, $\int D : \int P$ ratios decreased progressively from E1 to E5 and showed low values at the most productive stations E4W, A3 and F. Here, $\int D : \int P$ ratios were similar to those measured in nutrient-replete conditions such as productive upwelling regions (Brzezinski et al., 2003).

High $\int D : \int P$ ratios in winter and in early spring indicate that silica dissolution is sufficient to sustain a large fraction of the low Si uptake rates observed during non-bloom conditions and during the bloom onset, i.e. when primary production is still low. Indeed there is a temporal decoupling between silica production and dissolution since the dissolution kinetic is slow. It is only after diatom death and removal of their protecting organic coating by micro-organisms that the silica frustules can dissolve (Bidle and Azam, 1999; Bidle et al., 2003; Kamatani, 1982). By contrast, the progressive decrease of the $\int D : \int P$ values implies that the majority of gross silica production is sustained by the silicic acid pool supplied from below (winter water) as the bloom develops. This pool can be regarded as the “new” Si reservoir, similar to nitrate for N. Thus, we observe a seasonal shift from Si uptake behaving mainly as a regenerated production before the bloom onset, when silica production is still very low, and then behaving more like a new production during bloom, when we observe higher Si uptake rates.

An opposite shift at the end of the productive period was suggested by Brzezinski et al. (2001) in the upwelling system of the Monterey Bay with $\int D : \int P$ ratios increasing following the bloom development. In this case, higher $\int D : \int P$ values were associated

Seasonal evolution of net and regenerated silica production

I. Closset et al.

Title Page

Abstract

Introduction

Conclusions

References

Tables

Figures



Back

Close

Full Screen / Esc

Printer-friendly Version

Interactive Discussion



to an increase of the relative proportion of detrital BSi in the water column. Similarly, the occurrence of an accumulation of dissolving BSi in subsurface following productive periods inducing a net loss of BSi in late summer ($\int D : \int P = 1.7$) was already identified in the Australian sector of the Southern Ocean (Fripiat et al., 2011b). Since KEOPS-2 took place at the start of the bloom and since there was no silica dissolution rate measured from KEOPS-1, such increase of $\int D : \int P$ ratio in the Kerguelen area at the end of the blooming season has not been observed but will be discussed in Sect. 4.5.

Because silica dissolution profiles were not significantly different from each other between all the KEOPS-2 bloom stations (Fig. 4b), it can be ruled out as a process explaining the variability in $\int D : \int P$ ratios. The observed decreasing trend of $\int D : \int P$ ratios was actually mainly driven by the increase of BSi production rates (from 3.09 ± 0.01 to 47.9 ± 0.4 $\text{mmolSi m}^{-2} \text{d}^{-1}$) and by the accumulation of living diatoms with high specific Si uptake rates in the euphotic layer (Table 2).

The fraction of silica production supported by new silicic acid is estimated by $1 - \int D : \int P$. During KEOPS-2 it ranged from -0.58 in the HNLC station, where we observed a net loss of biogenic silica, to a maximum of 0.91 above the plateau, where maximum production rates were recorded (A3, Table 3). When plotting $1 - \int D : \int P$ vs. gross silica production rate, Brzezinski et al. (2003) found that 8 regional estimates of this parameter representing a large range of ocean environments, fall along an hyperbolic curve and thus it might be possible to predict the strength of the silicon pump in a system based on its mean silica production. To obtain a zero-intercept of the curve satisfying the assumption that when the fraction of silica production supported by new silicic acid approaches 0, the production must also be 0, we have plotted the $1 - \int D : \int P$ as a function of the net silica production (instead of the gross production). The fitting in Fig. 6 has been obtained on KEOPS-2, Brzezinski et al. (2003) and Fripiat et al. (2011b) data. Because the equation of the model fitting all the data follows a rectangular hyperbola, we can identify several parameters characterizing the distribution of both KEOPS-2 stations and other oceanic regions. The $1 - \int D : \int P_{\text{max}}$ is centered around 1 as it is not possible to have more than 100% of silica production supported

by new- H_4SiO_4 . The $K_{\rho\text{Net}}$ ($5.89 \pm 2.24 \text{ mmol m}^{-2} \text{ d}^{-1}$) represents the value of net silica production where the system shifts from a regenerated to a new biogenic silica production (i.e., $1 - \int D : \int P = 0.5$). In stations showing a net silica production below $K_{\rho\text{Net}}$, the development of diatoms is mainly controlled by recycled sources of silicon, while above this value, the supply of new H_4SiO_4 is the main source of nutrients for biogenic silica production.

Remarkably, KEOPS-2 stations follow the same trend as that of Brzezinski et al. (2003) and encompass almost the full range of variability observed in very contrasting oceanic regions (e.g. HNLC, oligotrophic, coastal upwelling, river plume). Taking into account these considerations, it is possible to sort KEOPS-2 stations into specific groups based on their silicon cycle functioning:

- The “low activity stations” group includes the HNLC reference station R and station E3 that showed a net loss of BSi with negative values of $\int \rho\text{Si}_{\text{net}}$ or close to 0 (Fig. 5; Table 2). In Fig. 6, the HNLC station falls in the negative part of the hyperbolic curve, close to stations mainly characterized by detrital BSi dominance and where a release of silicon from dissolving BSi takes place following a productive period (e.g. the late summer SAZ-Sense station P2 located in the Polar Front Zone; Fripiat et al., 2011b). Despite its low iron concentration, the high $\int D : \int P$ ratio observed at R suggests that a short development of diatoms could have occurred before our sampling in agreement with Jacquet et al. (2014) and Dehairs et al. (2014). This kind of low diatom production in the HNLC area surrounding the Kerguelen Plateau has already been suggested at the end of summer by Mosseri et al. (2008). Since net silica dissolution is not sustainable, the values measured at R should necessarily represent conditions that prevail on a short period of time. Production and dissolution rates are indeed snapshot measurements over 24 h or 48 h. Although H_4SiO_4 concentrations were not limiting in surface waters, E3 was characterized by very low silica production that could be exclusively sustained by recycled silicic acid ($1 - \int D : \int P = 0.05$) and seemed to have approached steady state conditions as siliceous biomass cannot increase

Seasonal evolution of net and regenerated silica production

I. Closset et al.

Title Page

Abstract

Introduction

Conclusions

References

Tables

Figures



Back

Close

Full Screen / Esc

Printer-friendly Version

Interactive Discussion



**Seasonal evolution of
net and regenerated
silica production**

I. Closset et al.

in a system supported solely by regenerated silicic acid (Brzezinski and Nelson, 1989). This situation could be the result of a previous attempt to bloom that would have aborted due to the destabilization of the ML.

- The “starting-bloom” group is represented by station E1 that has been visited in the beginning of the KEOPS-2 cruise (early November). Although carbon incubation experiments reveal that the bloom began to grow at this station (Cavagna et al., 2014), low Si uptake (Fig. 4a) and low net-silica production (Fig. 5) were still observed. A moderate $1 - \int D : \int P$ ratio (0.58) indicates that BSi production at E1 is controlled both by new and regenerated sources of H_4SiO_4 .
- The “spring-bloom” group includes stations holding a strong capacity for BSi accumulation, i.e. with low dissolution rates and high net silica production rates. Figure 4a allows us to distinguish between stations from the lagrangian study E4E and E5, with only moderate surface ρSi values (respectively $0.62 \pm 0.06 \mu\text{mol L}^{-1} \text{d}^{-1}$ and $0.57 \pm 0.06 \mu\text{mol L}^{-1} \text{d}^{-1}$) and $\int D : \int P$ ratio close to 0.3 (Table 3); and stations A3, F and E4W showing particularly high surface production rates ($> 1 \mu\text{mol L}^{-1} \text{d}^{-1}$) and $\int D : \int P$ ratio close to 0.1 (Table 3). Blooms with such a low $\int D : \int P$ ratio have the potential to accumulate a large fraction of BSi production and/or export a large amount of BSi into the deep ocean (Quéguiner, 2013; Tréguer and De La Rocha, 2013). Despite their location on both sides of the Polar Front and in different part of the Kerguelen bloom, stations E4W and F fall close to each other along the hyperbolic curve (Fig. 6). Consequently, they should operate in a comparable way in term of silica production dynamic which is quite similar to the average value of PFZ spring bloom conditions measured by Brzezinski et al. (2001). So, even though complex physical settings (Park et al. 2014) are very different between E4W (which is not part of PF with high surface DSi concentration of $17 \mu\text{mol L}^{-1}$) and F (with low surface DSi concentration of $6 \mu\text{mol L}^{-1}$) diatom production regime behave as typical PFZ stations. This was also observed with carbon export and mesopelagic remineralization by Jacquet et al. (2014).

[Title Page](#)[Abstract](#)[Introduction](#)[Conclusions](#)[References](#)[Tables](#)[Figures](#)[Back](#)[Close](#)[Full Screen / Esc](#)[Printer-friendly Version](#)[Interactive Discussion](#)

Seasonal evolution of net and regenerated silica production

I. Closset et al.

[Title Page](#)

[Abstract](#)

[Introduction](#)

[Conclusions](#)

[References](#)

[Tables](#)

[Figures](#)

[◀](#)

[▶](#)

[◀](#)

[▶](#)

[Back](#)

[Close](#)

[Full Screen / Esc](#)

[Printer-friendly Version](#)

[Interactive Discussion](#)



Compared to F and E4W, A3 is highly active in term of silica production and can be compared to the Amazon river plume and coastal upwelling systems such as Monterey Bay or Peru. This highlights once again the exceptional character of diatoms-dominated ecosystems sustained by natural iron fertilization in the Southern Ocean.

4.2 Decoupling between Si, C and N cycles in the Kerguelen area

In the Kerguelen area, the high NO_3^- concentrations in surface waters compared to H_4SiO_4 depletion observed annually at the end of the bloom period suggest a strong decoupling between the seasonal consumption of these two nutrients (Mosseri et al., 2008). This situation could be partly induced by differential recycling processes between Si and N strengthening the silicon pump. Si is thus primarily exported to deeper water through sinking of biogenic silica while PON is mostly recycled in the ML and used as nitrogen source for the development of new phytoplankton organisms including diatoms. Since organic matter is more quickly and efficiently remineralized compared to silica, this decoupling also occurs between Si and C.

The strength of the silicon pump could be investigated by comparing the Si : C and Si : N uptake-ratios. In this study, we use only the gross uptake ratios ($\int \rho\text{Si} : \int \rho\text{N}$ and $\int \rho\text{Si} : \int \rho\text{C}$), calculated as respectively:

$$\int \rho\text{Si} : \int \rho\text{N} = \frac{\rho\text{Si}}{\rho(\text{NO}_3^- + \text{NH}_4^+)} \quad (9)$$

and

$$\int \rho\text{Si} : \int \rho\text{C} = \frac{\rho\text{Si}}{\text{gross}\rho\text{C}} \quad (10)$$

which reflect only the stoichiometry of phytoplankton nutrient uptake. We will not consider net uptake ratios that could be calculated but would be biased by the significant

rates of nitrification estimated at all KEOPS-2 stations (see Cavagna et al., 2014 and Dehairs et al., 2014). Note that both $\int \rho \text{Si} : \int \rho \text{C}$ and $\int \rho \text{Si} : \int \rho \text{N}$ uptake ratios are underestimates of actual diatom uptake ratios because of the simultaneous C and N uptake by non-siliceous organisms. Diatoms growing in nutrient replete conditions present Si:C and Si:N elemental ratios around 0.13 (from 0.09 to 0.15) and 1 (from 0.8 to 1.2) respectively, with the variability of these ratios depending on diatom species, size classes and growth rates (Brzezinski, 1985; Martin-Jézéquel et al., 2000).

Si:C and Si:N uptake ratios are strongly impacted by co-limitations which alter growth rates and in most cases increase silicification processes, and thus lead to higher uptake ratios (Claquin et al., 2002; Leynaert et al., 2004; Bucciarelli et al., 2010). During the KEOPS-2 study, $\int \rho \text{Si} : \int \rho \text{C}$ and $\int \rho \text{Si} : \int \rho \text{N}$ uptake ratios vary from 0.10 to 0.38 and from 0.32 to 1.51 respectively (Table 3). Surprisingly, higher uptake ratios than those estimated by Brzezinski (1985) were found in stations with optimal nutrient conditions for diatom growth (e.g. A3) while lower uptake ratios were measured only at R, E3 and F. The main limiting factors reported for diatoms growth in the Southern Ocean that could explain these variations are the availability of macronutrients (such as silicic acid; Nelson and Tréguer, 1992; Quéguiner, 2001), light (Nelson and Smith, 1991) and micronutrients (especially iron; Boyd, 2002). Using a stoichiometric approach, we will identify in the following which processes mainly constrain the links between Si, N and C biogeochemical cycles in the different Kerguelen productive areas, and thus have an impact on the silicon pump functioning.

4.2.1 Influence of surface macronutrient concentrations on Si uptake rates

KEOPS-2 took place at the beginning of the growth period (October–November) and a bloom onset was observed above the Plateau (Blain et al., 2014). It is thus not surprising that macronutrient concentrations in the surface layer were not limiting for diatom growth (cf. Cavagna et al., 2014 for N uptake). For silicic acid, kinetic experiments conducted during the cruise at all sites demonstrated the lack of response of phytoplankton to H_4SiO_4 enrichment (data not shown). Indeed, at all stations, mixed layer silicic acid

BGD

11, 6329–6381, 2014

Seasonal evolution of net and regenerated silica production

I. Closset et al.

Title Page

Abstract

Introduction

Conclusions

References

Tables

Figures

◀

▶

◀

▶

Back

Close

Full Screen / Esc

Printer-friendly Version

Interactive Discussion



concentrations were high (from 6.2 to 18.5 μmolL^{-1} ; Fig. 3) preventing limitation of biogenic silica production by H_4SiO_4 availability.

4.2.2 Role of light limitation in the decoupling between Si and C

Results from a previous cruise in the same area (austral spring 1995) already highlighted the crucial role played by the light-mixing regime on the control of diatom growth in the nutrient replete waters (Blain et al., 2001). Indeed, even when iron is present at concentrations high enough to support optimum phytoplankton growth rates, the biomass in the ML could not increase in stations where unfavourable light-mixing regime was taking place due to either strong winds or mesoscale activity associated to the Polar Front. Light-limitation also takes part in the decoupling between Si, N and C cycles by decreasing the growth rate and consequently increasing Si : N and Si : C uptake-ratios. This is because the major uptake of silicon occurs during a different phase of the cell cycle (G2 + M) than photosynthesis and because this process is independent from the requirements of the other elements (Claquin et al., 2002).

At all stations the $\rho\text{Si} : \rho\text{C}$ uptake ratios increase slightly with depth and reach a maximum at the bottom of the euphotic layer (data not shown), in agreement with the fact that C assimilation is light-dependent through photosynthesis while silicification processes mainly involves energy coming from respiration (Martin-Jézéquel et al., 2000; Claquin et al., 2002). However, because Si uptakes reach very low values at the base of the euphotic layer (Fig. 4a), our data suggest that BSi production rates were not fully independent of light levels and that there was a close coupling between C and Si assimilation processes (see Cavagna et al., 2014 for carbon uptake). Indeed, both chlorophyll *a* and biogenic silica were still in substantial concentrations below the euphotic layer (e.g. $> 2 \text{ mg m}^{-3}$ and $> 3.5 \mu\text{molL}^{-1}$ respectively at A3; Fig. 3) indicating the presence of fresh siliceous phytoplankton cells. These observations suggested the occurrence of a subsurface accumulation of weakly active diatoms (Si uptakes $< 0.17 \mu\text{molSiL}^{-1} \text{ d}^{-1}$ and C-uptake $< 0.15 \mu\text{molCL}^{-1} \text{ d}^{-1}$ at A3). Such situation could be induced by deep-

BGD

11, 6329–6381, 2014

Seasonal evolution of net and regenerated silica production

I. Closset et al.

Title Page

Abstract

Introduction

Conclusions

References

Tables

Figures

◀

▶

◀

▶

Back

Close

Full Screen / Esc

Printer-friendly Version

Interactive Discussion



ening of the MLD which brings phytoplankton in the dark, limiting their growth. Indeed, in the Southern Ocean, the stratification of the upper water column is relatively weak and strong winds contribute to create punctually deep mixed layers as observed at A3 (Fig. 3e). Lower growth rates reach there a threshold that could strongly reduce the silicification processes. Actually even if in vitro incubations have clearly shown the decoupling of photosynthesis and silicification processes within a cell cycle (Claquin et al., 2002), this does not imply that they are strictly independent, especially when diatoms are brought to low-light environments.

4.2.3 Impact of iron on Si : N and Si : C uptake ratios

Limitation by trace metals (especially iron) also alters the stoichiometry of phytoplankton nutrient uptake and its elemental composition and, eventually, contributes to the decoupling between Si, N and C cycles. From bottle enrichment experiments, it has been argued that diatoms have higher Si : N uptake ratios under Fe stress (Takeda, 1998; Hutchins and Bruland, 1998; Franck et al., 2000). Interestingly, relatively high $\int \rho_{Si} : \int \rho_N$ ratios were measured for the Kerguelen spring bloom (Table 3), with the highest value above the Plateau (1.5, station A3) although this area was naturally Fe-enriched (Sarhou et al., 2014; Queroue et al., 2014). In the KEOPS-2 productive stations, diatoms can take up more H_4SiO_4 compared to nitrogen and carbon. Indeed, these organisms are known to store silicic acid in their vacuoles or linked to other intracellular components (Martin-Jézéquel et al., 2000; Hildebrand, 2008), or could be more silicified.

Thus, at a seasonal scale, the combination of this extra Si uptake and nitrogen regeneration processes including nitrification (see e.g. in Cavagna et al., 2014; Dehairs et al., 2014) in the beginning of the bloom, and preferential recycling of organic matter at the bloom offset helps to explain the depletion of most of the Si from surface layer observed between early spring ($18.7 \mu\text{mol L}^{-1}$, averaged in the upper 80 m at station A3, KEOPS-2) and the end of summer ($1.9 \mu\text{mol L}^{-1}$, averaged in the upper 80 m at station A3, KEOPS-1; Mosseri et al., 2008), while nitrate remains abundant ($23 \mu\text{mol L}^{-1}$,

BGD

11, 6329–6381, 2014

Seasonal evolution of net and regenerated silica production

I. Closset et al.

Title Page

Abstract

Introduction

Conclusions

References

Tables

Figures

◀

▶

◀

▶

Back

Close

Full Screen / Esc

Printer-friendly Version

Interactive Discussion



averaged in the upper 80 m at station A3, KEOPS-1; Mosseri et al., 2008). Non Fe-stressed diatom assemblages, such as those found at A3 (Sarhou et al., 2014), will deplete silicic acid from the water column before nitrate. Such silicon pump above Kerguelen Plateau would then not be driven solely by Fe-limitation contrary to incubation experiments from coastal upwelling systems (Hutchins and Bruland, 1998).

By contrast, 3 stations showed low $\int \rho\text{Si} : \int \rho\text{N}$ uptake ratios (0.44, 0.74 and 0.32 for R, E3 and F respectively). Lower Si : N and Si : C integrated uptake ratios in these areas might be partly due to changes in phytoplankton composition. Since the phytoplankton community at F may contain a significant fraction of non-siliceous organisms (data not shown), the C and N uptake ratios were not solely prescribed by diatoms and thus resulted in uptake ratios far below those expected for a plankton assemblage dominated by diatoms. Lower uptake ratios, as observed north of the Polar Front (station F, respectively 0.1 and 0.32; Table 3), suggest lower diatom contribution to primary production. Indeed, in contrast to the highest net silica production rates measured above the Plateau (Figs. 4a and 5), Cavagna et al. (2014) measured higher carbon assimilation north of the Polar Front (station F, $285 \pm 12 \text{ mmol m}^{-2} \text{ d}^{-1}$) than above the Plateau (station A3, $158 \pm 15 \text{ mmol m}^{-2} \text{ d}^{-1}$). Moreover, diatom assemblages at F were different from those found at A3, and could be composed mainly by less-silicified species. Indeed, previous studies in the Southern Ocean has already shown that diatom community composition could explain more differences in silicification than physiological responses to environmental factors as iron concentration (Baines et al., 2010; Assmy et al., 2013). In the same way and despite their location south of the Polar Front, the lower gross- $\int \rho\text{Si} : \int \rho\text{N}$ uptake ratios observed at stations R and E3 and are very similar to those measured by Brzezinski et al. (2003) in another Southern Ocean HNLC region with similar nutrient contents (≈ 0.7). In our case, they could be attributed to the occurrence of nanophytoplankton diatoms (i.e. smaller than $20 \mu\text{m}$, 59.4 % and 52.5 % of the siliceous biomass for R and E3 respectively; Lasbleiz et al., 2014).

BGD

11, 6329–6381, 2014

Seasonal evolution of net and regenerated silica production

I. Closset et al.

Title Page

Abstract

Introduction

Conclusions

References

Tables

Figures



Back

Close

Full Screen / Esc

Printer-friendly Version

Interactive Discussion



4.2.4 Implications for the Silicic acid leakage hypothesis

The silicon pump occurring in the Southern Ocean results in an Antarctic Surface Water (AASW) relatively replete in NO_3^- but strongly depleted in H_4SiO_4 as observed by Blain et al. (2007) and Mosseri et al. (2008) in the Kerguelen region. This property is then exported toward lower latitudes by the Antarctic Intermediate Water (AAIW) and Subantarctic Mode Water (SAMW) (Sarmiento et al., 2004), favouring non siliceous organisms production in these regions. Thus, any change in Si : N uptake ratios south of the region of AAIW and SAMW formation might in turn modify diatom productivity at low latitude. Matsumoto et al. (2002) proposed that a silicic acid leakage hypothesis (SALH) could explain the drop of atmospheric $p\text{CO}_2$ during glacial times and would be mainly driven by changes in Si : N ratios of diatoms induced by an increase in iron supply to the Southern Ocean. This hypothesis is based on *in vitro* and artificial Fe-enrichment experiments showing lower Si : N uptake ratios for diatoms in non Fe-stressed conditions (Takeda, 1998; Hutchins and Bruland, 1998), so that the increase of Fe-deposition in the Southern Ocean during glacial times would drive AASW towards NO_3^- depletion instead of the actual H_4SiO_4 depletion (Brzezinski et al., 2002).

As discussed previously, during KEOPS-2 we observe the opposite trend (Table 3): diatoms in Fe-replete conditions show higher $\int \rho\text{Si} : \int \rho\text{N}$ (e.g. 1.51 at A3) compared to those in the HNLC area (0.44 at R). This is also observed to a lesser extent at E3 where Fe incubation experiments have shown mild Fe limitation (Sarhou et al., 2014) and where we measured lower $\int \rho\text{Si} : \int \rho\text{N}$ (0.74) compared to A3. We may attribute this unexpected observation to the different diatom populations identified in these stations and especially to the dominance of different diatom size classes between R and A3 (Lasbleiz et al., 2014). Indeed, Fe enrichments in bottle experiments fertilise on short time scale (days) a diatom community that is not adapted to higher Fe levels. Here, by comparing $\int \rho\text{Si} : \int \rho\text{N}$ uptake ratios on different natural communities adapted to their specific ambient Fe levels, we show that natural Fe fertilisation favours diatoms with higher Si : N ratios. Above the Kerguelen Plateau, diatoms seem to maintain a relatively

BGD

11, 6329–6381, 2014

Seasonal evolution of net and regenerated silica production

I. Closset et al.

Title Page

Abstract

Introduction

Conclusions

References

Tables

Figures



Back

Close

Full Screen / Esc

Printer-friendly Version

Interactive Discussion



higher degree of silicification until the demise of the bloom, since Mosseri et al. (2008) observed the same range of $\int \rho \text{Si} : \int \rho \text{N}$ at A3 (1.6 ± 0.5 , $n = 3$).

Thus, in the iron-rich conditions of glacial periods, such diatoms populations would be able to maintain a similar nutrient uptake stoichiometry. This suggests that glacial Fe fertilization may not have necessarily resulted in a decrease in Si : N uptake ratios in AASW contrary to what has been proposed as an explanation for the SALH (Brzezinski et al., 2002). Other processes leading to SALH could be invoked, such as shifts in AAIW and SAMW formation rates (Crosta et al., 2007), variations in phytoplankton assemblages (including relative contribution of non-siliceous organisms) or changes in NO_3^- remineralization efficiency. However, further investigations concerning the seasonality of net silica production and Si : N uptake ratios in both naturally Fe-fertilized and HNLC areas of the Southern Ocean are clearly needed to support this observation.

4.3 Seasonality and budget of the silicon cycle above the Kerguelen Plateau

In order to investigate the seasonal evolution of Si biogeochemical cycle in the Kerguelen iron-fertilized bloom (station A3), we combined in Fig. 7 the KEOPS-1 and KEOPS-2 silicon fluxes measured using different isotopic approaches (stable and radiogenic isotope tracer incubations: ^{30}Si and ^{32}Si respectively, and, natural silicon isotopic composition, $\delta^{30}\text{Si}$, of both diatoms and seawater). Assuming that the whole water mass above the Kerguelen Plateau may have been significantly ventilated with surface waters from the HNLC area at the annual scale, Fripiat et al. (2011a) used the HNLC winter water (WW) characteristics to represent the initial conditions of the winter H_4SiO_4 stock in the fertilized area surface layer (0–100 m). Because the biological activity (Si and C assimilation) took place only in the upper 80 m during KEOPS-2, Si fluxes, stocks and values estimated by Fripiat et al. (2011a) discussed in this section were recalculated from the surface to 80 m (instead of 100 m in Fripiat et al., 2011a). The winter supply of DSi estimated from the seasonal H_4SiO_4 depletion during KEOPS-1 from the Upper Deep Circumpolar Water (UDCW) to the WW is around 2 mol m^{-2} , which is not signif-

Seasonal evolution of net and regenerated silica production

I. Closset et al.

Title Page

Abstract

Introduction

Conclusions

References

Tables

Figures

◀

▶

◀

▶

Back

Close

Full Screen / Esc

Printer-friendly Version

Interactive Discussion



BGD

11, 6329–6381, 2014

Seasonal evolution of net and regenerated silica production

I. Closet et al.

[Title Page](#)[Abstract](#)[Introduction](#)[Conclusions](#)[References](#)[Tables](#)[Figures](#)[⏪](#)[⏩](#)[◀](#)[▶](#)[Back](#)[Close](#)[Full Screen / Esc](#)[Printer-friendly Version](#)[Interactive Discussion](#)

icantly different from the 1.9 mol m^{-2} DSi stock we measured by mid-October during KEOPS-2 (1st visit at A3). This confirms that, as suggested by Fripiat et al. (2011a), the HNLC winter water is representative of the Si source with initial Si pool conditions prevailing before the bloom onset in the fertilized area. At this time, silica production (which was not measured during this 1st visit) should be very low since only little BSi accumulation was observed in the ML (79.1 mmol m^{-2}), and only $2 - 1.9 = 0.1 \text{ mol m}^{-2}$ of H_4SiO_4 was consumed in the surface water before our sampling compared to the estimated WW initial stock. The system was likely exclusively driven by regenerated silica production inducing a potentially high $\int D : \int P$ ratio (close to 1). Irradiance and mixed layer regime should be the more likely dominant factors controlling the bloom development for eukaryotes in winter and in early spring (Boyd et al., 2001; Blain et al., 2014). Models have previously reported that the interannual variability of mixed layer depth significantly affects both the date of the bloom onset and the maximum chlorophyll concentration in the region (Pondaven et al., 1998). Then, because H_4SiO_4 and Fe were not at limiting concentrations in the surface layer (Sarhou et al., 2014), the light-mixing regime that occurred above the Plateau by mid-October, should have been still unfavourable to diatom growth.

As the surface irradiance becomes more favourable with time, biogenic silica production progressively increases and reaches the highest net production value ($46.8 \text{ mmol m}^{-2} \text{ d}^{-1}$) measured during our 2nd visit to A3 (mid-November). Between these 2 samplings (i.e. during 28 days), the H_4SiO_4 depletion in the ML ($1.9 - 1.5 = 0.4 \text{ mol m}^{-2}$) yields to an average $\int \rho \text{Net}$ of $14.3 \text{ mmol m}^{-2} \text{ d}^{-1}$. Although it was located in different blooms of the Kerguelen region with different diatom communities, this value is in good agreement with the net silica production measured at station E1 which we characterized as a “starting-bloom” dynamic. Consequently, we can predict that simultaneously to the rise of silica production above the Plateau, the $\int D : \int P$ ratio should decrease toward values around 0.5 as measured at E1, and that the silica production could be controlled by both new and regenerated sources of H_4SiO_4 . In this situation, almost all the net BSi production is accumulated in the surface water: $348.5 \text{ mmol m}^{-2}$

Seasonal evolution of net and regenerated silica production

I. Closset et al.

Title Page

Abstract

Introduction

Conclusions

References

Tables

Figures



Back

Close

Full Screen / Esc

Printer-friendly Version

Interactive Discussion



(BSi stock integrated over 80 m, this study) and very low export of biogenic silica is allowed from the ML to the bottom layer: $4.7 \text{ mmol m}^{-2} \text{ d}^{-1}$ (estimated from the difference between net production calculated with DSi standing stocks and that calculated using BSi standing stocks, 14.3 and $9.6 \text{ mmol m}^{-2} \text{ d}^{-1}$ respectively). These observations are in good agreement with the low carbon export (4 % of the surface primary production) estimated during the first visit at A3 by Jacquet et al. (2014). Indeed, such early spring bloom generally starts by the development of lightly silicified diatoms with potentially low sedimentation rates (Quéguiner, 2013).

The H_4SiO_4 stock measured during the second visit at A3 (1.5 mol m^{-2}) can sustain the strong net silica production rates measured there for 32 days. Using natural Si isotopic approach, Fripiat et al. (2011a) suggested that diatoms could receive in addition, at least 1.2 mol m^{-2} of DSi coming from the WW during the productive period in the upper 80 m of the fertilized area, allowing 26 supplementary days of growth for diatoms with the same high Si uptake rate. Taking into account the sum of such winter and summer vertical Si supply, the high productive period as measured in A3 can be maintained during 86 days. Remarkably, this is almost similar to the estimation by Mongin et al. (2008) based on satellite products of 85 days of blooming over the Kerguelen Plateau. Using a box-model approach, De Brauwere et al. (2012) suggested that the bloom could also persist over the same duration without considering this summer Si supply from deep-waters. This appears unlikely because the high net silica production we measured at A3 could not be sustained for more than 32 days. Even if such high net silica production should probably not be representative of the Si uptake by diatoms over the Plateau during the rest of bloom period, an additional source of Si is needed. The very good accordance of our results with the bloom duration from Mongin et al. (2008) suggests that this summer H_4SiO_4 input in the ML is realistic and could sustain a significant part of the phytoplankton growth above the Kerguelen Plateau. Indeed, high internal wave activity above the plateau is assumed to be a major process for vertical dissolved iron (and other nutrients) supply on the upper waters (Park et al., 2008; Blain et al., 2008).

Seasonal evolution of net and regenerated silica production

I. Closset et al.

Title Page

Abstract

Introduction

Conclusions

References

Tables

Figures



Back

Close

Full Screen / Esc

Printer-friendly Version

Interactive Discussion



These vertical fluxes allow a 2-months period of highly active blooming, with a system controlled exclusively by new sources of H_4SiO_4 ($\int D : \int P = 0.09$, A3, Table 3), inducing the strong DSi depletion observed in January (DSi stocks at 0.2 mol m^{-2} , KEOPS-1; Mosseri et al., 2008) and the high BSi accumulation in the ML ($348.5 \text{ mmol m}^{-2}$, KEOPS-2; this study) which could be exported at the end of summer when the water column stratification becomes weaker. The gross- $\int \rho\text{Si}$ measured here is in the upper range of published values in the Southern Ocean and the specific Si uptake rate was relatively high (respectively $47.9 \text{ mmol m}^{-2} \text{ d}^{-1}$ and 0.28 d^{-1} in the euphotic layer; Table 2). This could indicate that diatoms have already reached their maximum BSi production rate, and that our second visit to A3 could represent the maximum of the bloom dynamic above the Plateau. This is quite consistent with the date of the bloom peak estimated in early December both by modeling and satellite approaches (De Brauwere et al., 2012 and Mongin et al., 2008). The H_4SiO_4 standing stock in the ML would then be depleted by mid-January (0.2 mol m^{-2} , KEOPS-1; Mosseri et al., 2008). Then the bloom would shift toward a steady state dynamic, almost entirely controlled by regenerated Si with decreasing gross silica production down to $10.7 \text{ mmol m}^{-2} \text{ d}^{-1}$, KEOPS-1 (Mosseri et al., 2008) and where H_4SiO_4 concentration in the ML becomes limiting for diatom growth.

This progression of Si limitation could be associated to a change in the phytoplankton community as observed between the different visits at A3 during KEOPS-1 (Mosseri et al., 2008; Armand et al., 2008), and could be related to the selection of species with higher affinities with silicic acid resulting in a better ability to grow at low H_4SiO_4 concentrations. Such change in the community structure in response to physical and biological forcing was also proposed in a conceptual scheme by Quéguiner (2013). In spring, diatoms presenting high growth rates and low degree of silicification dominate the bloom which development is mainly controlled by new nutrients sources. This diatom assemblage will be soon affected by the availability of both silicic acid and iron, and will change for a population showing lower growth rates exclusively sustained by regenerated sources of H_4SiO_4 . This second assemblage, beginning to dominate in

Seasonal evolution of net and regenerated silica production

I. Closset et al.

Title Page

Abstract

Introduction

Conclusions

References

Tables

Figures

◀

▶

◀

▶

Back

Close

Full Screen / Esc

Printer-friendly Version

Interactive Discussion



January, could thus persist at steady state until May, when PAR decreases below the threshold of $1 \text{ mol photon m}^{-2} \text{ d}^{-1}$ (Blain et al., 2014) in waters that are quite depleted in H_4SiO_4 , as it is composed by small diatoms with high affinities for silicic acid (Mosseri et al., 2008) and a deep silica maximum (DSM) characterized by strongly silicified large-sized diatoms growing at the base of the ML in the nutrient gradient (Quéguiner, 2013). Under such conditions, a very low net silica production and a $\int D : \int P$ ratio close to 1 are expected. Unfortunately no silica dissolution measurements are available from KEOPS-1. However, we can try to estimate the net production from the difference between the KEOPS-1 average gross silica production ($10.7 \text{ mmol m}^{-2} \text{ d}^{-1}$; Mosseri et al., 2008) and average silica dissolution measured at all stations south of the Polar Front during KEOPS-2 ($10.2 \text{ mmol m}^{-2} \text{ d}^{-1}$). The choice of a constant silica dissolution rate throughout the productive season may seem surprising. However, there are several reasons to support this hypothesis: (i) Brzezinski et al. (2001) show that the seasonal variability of silica dissolution rates in the Southern Ocean is very low ($6.7 \text{ mmol m}^{-2} \text{ d}^{-1}$ in October/November to $6.6 \text{ mmol m}^{-2} \text{ d}^{-1}$ in February/March); (ii) $\int \rho \text{Diss}$ measured close to the Polar Front by Fripiat et al. (2011b) in late summer were very close to our spring dissolution values (4.9 to $6.6 \text{ mmol m}^{-2} \text{ d}^{-1}$). (iii) As best seen on Fig. 4b, all KEOPS-2 stations except the HNLC one (R) have similar silica dissolution profiles. Thus it is reasonable to assume that the net silica production estimated above the plateau in late summer should be around $0.5 \text{ mmol m}^{-2} \text{ d}^{-1}$ (Fig. 7).

The BSi standing stock observed in the upper layer in late summer ($275.3 \text{ mmol m}^{-2}$, KEOPS-1; Mosseri et al., 2008) is lower than that measured in spring ($348.5 \text{ mmol m}^{-2}$). This could indicate that a part of the BSi that was produced before reaching a silica production in steady state (i.e. sustained almost entirely by regenerating production) was not accumulated in the surface ML at the end of the productive period. In fact, a part of the summer production can be stocked in the form a DSM as measured in late summer above the plateau ($550.1 \text{ mmol m}^{-2}$ between 100 and 200 m; Mosseri et al., 2008) which was not yet present at KEOPS-2. This subsurface biogenic silica accumulation mainly results from the combination of sedi-

mentation of living but inactive cells and the occurrence of phytoplankton populations living at depth (Uitz et al., 2009; Fripiat et al., 2011a). The part of the summer net silica production which is not accumulated below the ML should thus be exported to deeper waters as the seasonal stratification breaks down with the intensification of vertical mixing. In term of carbon export, this flux could represent 14 to 31 % of the surface primary production (KEOPS-1, station A3; Jacquet et al., 2008). As proposed by Quéguiner (2013), a massive export of biogenic silica and organic matter ($58 \text{ days} \times 46.8 \text{ mmol m}^{-2} \text{ d}^{-1} - (275.3 + 550 \text{ mmol m}^{-2}) = 2.2 \text{ mol Si m}^{-2}$) should occur and could then represent the major annual event of the silicon and biological carbon pumps.

Although our budget of the silicon biogeochemical cycle above the Kerguelen Plateau is based on different silicon isotopic approaches and is sustained by silicon stocks and fluxes coming from different years, it matches very well with all the previous individual findings. The seasonal variations of $\int D : \int P$ ratio are in accordance with those observed by Brzezinski et al. (2001) across the Polar Front Zone and are quite well represented by the recent model of Coffineau et al. (2013), who estimate a $\int D : P$ ratio ranging from 0.64 in winter to 0.19 during the spring bloom. The good accordance of our approach with outcomes from different studies also highlights that, to fully characterize the silicon cycle in a region of interest, we need to measure both silica production and dissolution rates. Indeed, taking only into account the gross silica production in such a synthesis exercise (i.e. without measuring silica dissolution as it is the case in most studies) could lead to misinterpretations of the silicon pump functioning. For instance, we would not be able to identify shifts between “new” and “regenerated” silica production neither to accurately calculate the real bloom duration without considering silica recycling. Without taking into account dissolution, silica production would have been overestimated by 21 % in the mixed layer ($58.2 \text{ mmol m}^{-2} \text{ d}^{-1}$ compared to the $47.9 \text{ mmol m}^{-2} \text{ d}^{-1}$ of real net silica production), and the bloom duration computation would have yielded 74 days, which is not consistent with the 85 days of KEOPS-1 bloom duration observed by Mongin et al. (2008).

Seasonal evolution of net and regenerated silica production

I. Closset et al.

Title Page

Abstract

Introduction

Conclusions

References

Tables

Figures



Back

Close

Full Screen / Esc

Printer-friendly Version

Interactive Discussion



5 Conclusions

Our study addressed the seasonal evolution of the efficiency of the silicon pump and of the biogenic silica fluxes in the mixed layer under different naturally iron-fertilized bloom conditions around the Kerguelen region. Integrated Si uptake rates were among the highest reported so far in the Southern Ocean. They varied from $3.09 \pm 0.01 \text{ mmol m}^{-2} \text{ d}^{-1}$ in the HNLC area (R) to $47.9 \pm 0.4 \text{ mmol m}^{-2} \text{ d}^{-1}$ above the plateau (A3) and seemed to be strongly coupled with C uptake over depth. Indeed, C and Si assimilation were very low below the euphotic layer indicating the occurrence of a subsurface accumulation of living but inactive diatoms. Although significant, silica dissolution rates were generally much lower than production rates and did not vary between bloom stations nor over depth.

We observed a shift from a BSi production regime based on the regeneration of H_4SiO_4 during the early stages of bloom onset (with an averaged $\int D : \int P$ ratio of 0.98) to a regime based on new production during the bloom development (with an averaged $\int D : \int P$ ratio of 0.18). This change switched on an active silicon pump which led to the decoupling between Si and N cycles as well as a strong H_4SiO_4 depletion of surface water by late summer, with significant implications for global biogeochemical properties. Indeed, the system progressively shifted toward a stronger silicon pump as Si uptake rates increased and nitrogen became preferentially remineralized when the bloom was well established. This led ultimately to a strong Si limitation and drove the system toward a regenerated silica production regime which allowed the persistence of the bloom in a steady state despite the low concentrations of silicic acid concentrations. Our results confirm and complete the concept of a seasonal transition from a diatom new production to a diatom regenerated production already proposed in the Antarctic Zone by Brzezinski et al. (2003).

Moreover, in opposition to previous artificial Fe-enrichment bottle experiments outcomes, Si:N and Si:C uptake ratios during KEOPS-2 were not higher in the HNLC area compared to the fertilized region. This observation could have great implica-

BGD

11, 6329–6381, 2014

Seasonal evolution of net and regenerated silica production

I. Closset et al.

Title Page

Abstract

Introduction

Conclusions

References

Tables

Figures

⏪

⏩

◀

▶

Back

Close

Full Screen / Esc

Printer-friendly Version

Interactive Discussion



Seasonal evolution of net and regenerated silica production

I. Closset et al.

Title Page

Abstract

Introduction

Conclusions

References

Tables

Figures



Back

Close

Full Screen / Esc

Printer-friendly Version

Interactive Discussion



tions on our understanding on processes involved in setting atmospheric $p\text{CO}_2$ during glacial-interglacial transitions. Our results suggest that the increase of low latitude diatom production observed during glacial periods should not be controlled primarily by a shift in the nutrient uptake stoichiometry of Antarctic diatoms induced by an enhanced iron supply, as proposed in the silicic acid leakage hypothesis (Matsumoto et al., 2002; Brzezinski et al., 2002), but further investigations are clearly needed to support this idea.

The combination of the results from the two KEOPS cruises (early spring and late summer) and of different isotopic approaches, allowed the first seasonal estimate of a closed silicon biogeochemical budget in the iron-fertilized area above the Kerguelen Plateau based on direct measurements. Our estimates emphasize the interest of combining different tracers and methods with different sensitivities to physical and biological processes to better constrain and quantify all the processes simultaneously. The major outcome of this seasonal budget is that the winter and summer silicon supplies to the mixed layer ($3.2 \text{ mol m}^{-2} \text{ yr}^{-1}$) seem to be well balanced by the combination of biogenic silica accumulation (both in the upper layer and in the winter waters) and late summer BSi export (respectively $0.3 + 0.6 + 2.2 = 3.1 \text{ mol m}^{-2} \text{ yr}^{-1}$). This confirms the occurrence of a significant summer Si supply from Winter Water as suggested by Fripiat et al. (2011a) sustaining the diatom bloom over the Kerguelen Plateau.

Finally, the most striking feature of this study is that naturally iron fertilized areas of the Southern Ocean, like the Kerguelen Plateau, could sustain a biogenic silica production regime similar to those observed in coastal upwelling systems or in large river plume. This highlights the exceptional character of diatoms-dominated ecosystems associated to natural iron fertilization in the Southern Ocean, and their significant role in the global Si biogeochemical cycle. Even if the outcomes of this budget are consistent with previous measurements, large uncertainties remain about the seasonal evolution of dissolution rates at the end of the productive period. Indeed, in order to fully characterize the Si-biogeochemical cycle in a region of interest, it is recommended to measure both BSi production and dissolution rates. In combination, the natural silicon

isotopic composition ($\delta^{30}\text{Si}$) of diatoms and seawater represents a powerful tool for identifying silicon sources and silica production over larger temporal and spatial scales (Fripiat et al., 2011a; Tréguer and De la Rocha, 2013), and will be also examined during KEOPS-2. The combination of several isotopic approaches, as well as modeling exercises (such as in Pondaven et al., 1998; De Brauwere et al., 2012; Coffineau et al., 2013), by allowing to better constrain and quantify different physical and biogeochemical processes simultaneously, would strongly improve our understanding of the regional Si biogeochemical cycle and its implications in the global ocean biogeochemistry.

Supplementary material related to this article is available online at

<http://www.biogeosciences-discuss.net/11/6329/2014/>

[bgd-11-6329-2014-supplement.pdf](#).

Acknowledgements. Authors would like to thank Stéphane Blain as the KEOPS-2 project coordinator, the captain and the crew of the R/V *Marion-Dufresne II* for assistance on board. We are also especially grateful to Luc André who has allowed the access to the HR-SF-ICP-MS at the Royal Museum of Central Africa. This work was supported by the French Research program of INSU-CNRS LEFE-CYBER (“Les enveloppes fluides et l’environnement” – “Cycles biogéochimiques, environnement et ressources”), the French ANR (“Agence Nationale de la Recherche”, SIMI-6 program), the French CNES (“Centre National d’Etudes Spatiales”) and the French Polar Institute IPEV (Institut Polaire Paul-Emile Victor). The research leading to these results has also received funding from the European Union Seventh Framework Programme under grant agreement n° 294146 (MuSiCC Marie Curie CIG).

References

- Armand, L., Cornet-Barthaux, V., Mosseri, J., and Quéguiner B.: Late summer diatom biomass and community structure on and around the naturally iron-fertilised Kerguelen Plateau in the Southern Ocean, *Deep-Sea Res. II*, 55, 653–676, 2008.
- Assmy, P., Smetacek, V., Montresor, M., Klaas, C., Henjes, J., Strass, V., Arrieta, J., Bathmann, U., Berg, G., Breitbarth, E., Cisewski, B., Friedrichs, L., Fuchs, N., Herndl, G., Jansen, S., Krägersky S., Latasa, M., Peeken, I., Röttgers R., Scharek, R., Schüller S.,

Seasonal evolution of net and regenerated silica production

I. Closset et al.

Title Page

Abstract

Introduction

Conclusions

References

Tables

Figures



Back

Close

Full Screen / Esc

Printer-friendly Version

Interactive Discussion



Seasonal evolution of net and regenerated silica production

I. Closset et al.

Title Page

Abstract

Introduction

Conclusions

References

Tables

Figures

◀

▶

◀

▶

Back

Close

Full Screen / Esc

Printer-friendly Version

Interactive Discussion



Steigenberger, S., Webb, A., and Wolf-Gladrow, D.: Thick-shelled, grazer-protected diatoms decouple ocean carbon and silicon cycles in the iron-limited Antarctic Circumpolar Current, *P. Natl. Acad. Sci. USA*, 110, 20633–20638, 2013.

Baines, S., Twining, B., Brzezinski, M., Nelson, D., and Fisher, N.: Causes and biogeochemical implications of regional differences in silicification of marine diatoms, *Global Biogeochem. Cy.*, 24, GB4031, doi:10.1029/2010GB003856, 2010.

Beucher, C., Tréguer P., Hapette, A. M., and Corvaisier, R.: Intense summer Si-recycling in the surface Southern Ocean. *Geophys. Res. Lett.*, 31, L09305, doi:10.1029/2003GL018998, 2004.

Bidle, K. D. and Azam, F.: Accelerated dissolution of diatom silica by marine bacterial assemblages, *Nature*, 397, 508–512, 1999.

Bidle, K. D., Brzezinski, M., Long, R., Jones, J., and Azam, F.: Diminished efficiency in the oceanic silica pump caused by bacteria-mediated silica dissolution, *Limnol. Oceanogr.*, 48, 1855–1868, 2003.

Blain, S., Tréguer P., Belviso, S., Bucciarelli, E., Denis, M., Desabre, S., Fiala, M., Martin-Jézéquel V., Le Fèvre J., Mayzaud, P., Marty, J.-C., and Razouls, S.: A biogeochemical study of the island mass effect in the context of the iron hypothesis: Kerguelen Islands, Southern Ocean, *Deep-Sea Res. I*, 48, 163–187, 2001.

Blain, S., Quéguiner B., Armand, L., Belviso, S., Bombled, B., Bopp, L., Bowie, A., Brunet, C., Brussaard, C., Carlotti, F., Christaki, U., Cordière A., Durand, I., Ebersbach, F., Fuda, J.-L., Garcia, N., Gerringa, L., Griffiths, B., Guigue, C., Guillerm, C., Jacquet, S., Jean-del, C., Laan, P., Lefèvre D., Lo Monaco, C., Malits, A., Mosseri, J., Obernosterer, I., Park, Y.-H., Picheral, M., Pondaven, P., Remenyi, T., Sandroni, V., Sarthou, G., Savoye, N., Scouarnec, L., Souhaut, M., Thuiller, D., Timmermans, K., Trull, T., Uitz, J., Van Beek, P., Velhuis, M., Vincent, D., Viollier, E., Vong, L., and Wagener, T.: Effect of natural iron fertilization on carbon sequestration in the Southern Ocean, *Nature*, 446, 1070–1075, 2007.

Blain, S., Quéguiner B., and Trull, T.: The natural iron fertilization experiment KEOPS (Kerguelen Ocean and Plateau compared Study): an overview, *Deep-Sea Res. II*, 55, 559–565, 2008.

Blain, S., Renaut, S., Xing, X., Claustre, H., and Guinet, C.: Instrumented elephant seals reveal the seasonality in chlorophyll and light-mixing regime in the iron fertilized Southern Ocean, *Geophys. Res. Lett.*, 40, 1–5, 2013.

Seasonal evolution of net and regenerated silica production

I. Closset et al.

[Title Page](#)

[Abstract](#)

[Introduction](#)

[Conclusions](#)

[References](#)

[Tables](#)

[Figures](#)

[◀](#)

[▶](#)

[◀](#)

[▶](#)

[Back](#)

[Close](#)

[Full Screen / Esc](#)

[Printer-friendly Version](#)

[Interactive Discussion](#)



- Blain, S.: KEOPS2: implementation and overview, Biogeosciences Discuss., in preparation, 2014.
- Boyd, P.: The role of iron in the biogeochemistry of the Southern Ocean and equatorial Pacific: a comparison of in situ iron enrichments, *Deep-Sea Res. II*, 49, 1803–1821, 2002.
- 5 Boyd, P., Crossley, A., DiTullio, G., Griffiths, F., Hutchins, D., Quéguiner B., Sedwick., and Trull, T.: Control of phytoplankton growth by iron supply and irradiance in the subantarctic Southern Ocean: experimental results from the SAZ Project, *J. Geophys. Res.*, 106, 31573–31583, 2001.
- 10 Boyd, P., Crossley, A., diTullio, G., Friffiths, F., Hutchins, D., Queguiner, B., Sedwick, P., and Trull, T.: Control of phytoplankton growth by iron supply and irradiance in the subantarctic Southern Ocean: experimental results from the SAZ Project, *J. Geophys. Res.*, 106, 31573–31583, 2007.
- Brzezinski, M.: The Si:C:N ratio of marine diatoms: interspecific variability and the effect of some environmental variables, *J. Phycol.*, 21, 347–357, 1985.
- 15 Brzezinski, M. and Nelson, D.: Seasonal changes in the silicon cycle within a Gulf Stream warm-core ring, *Deep-Sea Res.*, 36, 1009–1030, 1989.
- Brzezinski, M., Nelson, D., Franck, V., and Sigmon, D.: Silicon dynamics within an intense open-ocean diatom bloom in the Pacific sector of the Southern Ocean, *Deep-Sea Res. II*, 48, 3997–4018, 2001.
- 20 Brzezinski, M. A., Pride, C. J., Frank, V. M., Sigman, D. M., Sarmiento, J. L., Matsumoto, K., Gruber, N., Rau, G. H., and Coale, K. H.: A switch from Si(OH)₄ to NO₃-depletion on the glacial Southern Ocean, *Geophys. Res. Lett.*, 29, doi:10.1029/2001GL014349, 2002.
- Brzezinski, M., Jones, J., Bidle, K., and Azam, F.: The balance between silica production and silica dissolution in the sea: insights from Monterey Bay, California, applied to the global data set, *Limnol. Oceanogr.*, 48, 1846–1854, 2003.
- 25 Bucciarelli, E., Pondaven, P., and Sarthou, G.: Effects of an iron-light co-limitation on the elemental composition (Si, C, N) of the marine diatoms *Thalassiosira oceanica* and *Ditylum brightwellii*, *Biogeosciences*, 7, 657–669, doi:10.5194/bg-7-657-2010, 2010.
- Buesseler, K., Ball, L., Andrews, J., Cochran, J., Hirschberg, D., Bacon, M., Fler, A., and Brzezinski, M.: Upper ocean export of particulate organic carbon and biogenic silica in the Southern Ocean along 170° W, *Deep-Sea Res. II*, 48, 4275–4297, 2001.
- 30 Cavagna, A. J. Blain, S., Cardinal, D., Closset, I., Dehairs, F., Fernandez, C., Flores-Leive, L., Lasbleiz, M., Lefèvre D., Leblanc, K., and Quéguiner B.: Biological productivity regime and

Seasonal evolution of net and regenerated silica production

I. Closset et al.

Title Page

Abstract

Introduction

Conclusions

References

Tables

Figures



Back

Close

Full Screen / Esc

Printer-friendly Version

Interactive Discussion



in-situ methods comparison around the Kerguelen Island in the Southern Ocean. KEOPS 2 primary and community producers regime using various uptake rates and their stoichiometric ratios, Biogeosciences Discuss., in preparation, 2014.

5 Claquin, P., Martin-Jézéquel V., Kromkamp, J. C., Veldhuis, M. J. W., and Kraay, G. W.: Uncoupling of silicon compared to carbon and nitrogen metabolisms, and role of the cell cycle, in continuous cultures of *Thalassiosira pseudonana* (Bacillariophyceae) under light, nitrogen and phosphorus control, J. Phycol., 38, 922–930, 2002.

Coffineau, N., De La Rocha, C. L., and Pondaven, P.: Exploring interacting influences on the silicon isotopic composition of the surface ocean: a case study from the Kerguelen Plateau, Biogeosciences Discuss., 10, 11405–11446, doi:10.5194/bgd-10-11405-2013, 2013.

10 Corvaisier, R., Tréguer P., Beucher, C., and Elskens, M.: Determination of the rate of production and dissolution of biosilica in marine waters by thermal ionisation mass spectrometry, Anal. Chim. Acta, 534, 149–155, 2005.

15 Crosta, X., Beucher, C., Pahnke, K., and Brzezinski, M.: Silicic acid leakage from the Southern Ocean: opposing effects of nutrient uptake and oceanic circulation, Geophys. Res. Lett., 34, L13601, doi:10.1029/2006GL029083, 2007.

20 De Baar, H., Boyd, P., Coale, K., Landry, M., Tsuda, A., Assmy, P., Bakker, D., Bozec, Y., Barber, R., Brzezinski, M., Buesseler, K., Boye, M., Croot, P., Gervais, F., Gorbunov, M., Harrison, P., Hiscock, W., Laan, P., Lancelot, C., Law, C., Levasseur, M., Marchetti, A., Millero, F., Nishioka, J., Nojiri, Y., van Oijen, T., Riebesell, U., Rikenberg, M., Saito, H., Takeda, S., Timmermans, K., Veldhuis, M., Waite, A., and Wong, C.-S.: Synthesis of iron fertilization experiments: from the Iron Age in the Age of Enlightenment, J. Geophys. Res., 110, C09S16, doi:10.1029/2004JC002601, 2005.

25 De Brauwere, A., De Ridder, F., Elskens, M., Schoukens, J., Pintelon, R., and Baeyens, W.: Refined parameter and uncertainty estimation when both variables are subject to error, Case study: estimation of Si consumption and regeneration rates in a marine environment, J. Mar. Syst., 55, 205–221, 2005.

30 De Brauwere, A., Fripiat, F., Cardinal, D., Cavagna, A.-J., De Ridder, F., André, L., and Elskens, M.: Isotopic model of oceanic silicon cycling: the Kerguelen Plateau case study, Deep-Sea Res. I, 70, 42–59, 2012.

Dehairs, F., Trull, T., Fernandez, C., Davies, D., Cavagna, A. J., Planchon, F., and Fripiat, F.: Nitrate isotopic composition in the Kerguelen area (Southern Ocean) during KEOPS 2, Biogeosciences Discuss., in preparation, 2014.

- Dugdale, R., Wilkerson, F., and Minas, H.: The role of a silicate pump in driving new production, *Deep-Sea Res. I*, 5, 697–719, 1995.
- Elskens, M., de Brauwere, A., Beucher, C., Corvaisier, R., Savoye, N., Tréguer P., and Baeyens, W.: Statistical process control in assessing production and dissolution rates of biogenic silica in marine environments, *Mar. Chem.*, 106, 272–286, 2007.
- Franck, V., Brzezinski, M., Coale, K., and Nelson, D.: Iron and silicic acid concentrations regulate Si uptake north and south of the Polar Frontal Zone in the Pacific Sector of the Southern Ocean, *Deep-Sea Res. II*, 47, 3315–3338, 2000.
- Fripiat, F.: Isotopic approaches in the silicon cycle: The Southern Ocean case study (Ph.D. dissertation), Université Libre de Bruxelles, Brussels, 266 pp., 2010.
- Fripiat, F., Corvaisier, R., Navez, J., Elskens, M., Schoemann, V., Leblanc, K., André, L., and Cardinal, D.: Measuring production-dissolution rates of marine biogenic silica by ^{30}Si -isotope dilution using a high-resolution sector field inductively coupled plasma mass spectrometer, *Limnol. Oceanogr.*, 7, 470–478, 2009.
- Fripiat, F., Cavagna, A. J., Savoye, N., Dehairs, F., André, L., and Cardinal, D.: Isotopic constraints on the Si-biogeochemical cycle of the Antarctic Zone in the Kerguelen area (KEOPS), *Mar. Chem.*, 123, 11–22, 2011a.
- Fripiat, F., Leblanc, K., Elskens, M., Cavagna, A. J., Armand, L., André, L., Dehairs, F., and Cardinal, D.: Efficient silicon recycling in summer in both the Polar Frontal and Subantarctic Zones of the Southern Ocean, *Mar. Ecol.-Prog. Ser.*, 435, 47–61, 2011b.
- Hildebrand, M.: Diatoms, biomineralization processes, and genomics, *Chem. Rev.*, 108, 4855–4874, 2008.
- Hutchins, D. and Bruland, K.: Iron-limited diatom growth and Si:N uptake ratios in a coastal upwelling regime, *Nature*, 393, 561–564, 1998.
- Jacquet, S. H. M., Dehairs, F., Savoye, N., Obernosterer, I., Christaki, U., Monnin, C., and Cardinal, D.: Mesopelagic organic carbon remineralization in the Kerguelen Plateau region tracked by biogenic particulate Ba, *Deep-Sea Res. II*, 55, 868–879, 2008.
- Jacquet, S. H. M., Dehairs, F., Cavagna, A. J., Planchon, F., Monin, L., and André, L.: Early season mesopelagic carbon remineralization and transfer efficiency in the naturally iron-fertilized Kerguelen area, *Biogeosciences Discuss.*, in preparation, 2014.
- Kamatani, A.: Dissolution rates of silica from diatoms decomposing at various temperatures, *Mar. Biol.*, 68, 91–96, 1982.

Seasonal evolution of net and regenerated silica production

I. Closset et al.

Title Page

Abstract

Introduction

Conclusions

References

Tables

Figures

◀

▶

◀

▶

Back

Close

Full Screen / Esc

Printer-friendly Version

Interactive Discussion



Seasonal evolution of net and regenerated silica production

I. Closset et al.

Title Page

Abstract

Introduction

Conclusions

References

Tables

Figures

◀

▶

◀

▶

Back

Close

Full Screen / Esc

Printer-friendly Version

Interactive Discussion



- Karl, D. and Tien, G.: MAGIC: A sensitive and precise method for measuring dissolved phosphorus in aquatic environment, *Limnol. Oceanogr.*, 37, 105–116, 1992.
- Lasbleiz, M., Leblanc, K., Claustre, H., Uitz, J., Cornet-Barthaux, V., Ouhssain, M., Ras, J., and Quéguiner B.: Particulate matter distribution in relation to phytoplankton community structure in the Fe-fertilized Kerguelen region of the Southern Ocean during austral spring (KEOPS2), *Biogeosciences Discuss.*, in preparation, 2014.
- Leynaert, A., Bucciarelli, E., Claquin, P., Dugdale, R. C., Martin-Jézéquel V., Pondaven, P., and Ragueneau, O.: Effect of iron deficiency on diatom cell size and silicic acid uptake kinetics, *Limnol. Oceanogr.*, 49, 1134–1143, 2004.
- Martin-Jézéquel V., Hildebrand, M., and Brzezinski, M.: Silicon metabolism in diatoms: implications for growth, *J. Phycol.*, 36, 821–840, 2000.
- Matsumoto, K., Sarmiento, J. L., and Brzezinski, M. A.: Silicic acid leakage from the Southern Ocean: a possible explanation for glacial atmospheric $p\text{CO}_2$, *Global Biogeochem. Cy.*, 16, doi:10.1029/2001GB001442, 2002.
- Mongin, M., Molina, E., and Trull, T.: Seasonality and scale of the Kerguelen plateau phytoplankton bloom: a remote sensing and modeling analysis of the influence of natural iron fertilization in the Southern Ocean, *Deep-Sea Res. II*, 55, 880–892, 2008.
- Mosseri, J., Quéguiner B., Armand, L., and Cornet-Barthaux, V.: Impact of iron on silicon utilization by diatoms in the Southern Ocean: a case study of Si/N cycle decoupling in a naturally iron-enriched area, *Deep-Sea Res. II*, 55, 810–819, 2008.
- Nelson, D. and Goering, J. J.: A stable isotope tracer method to measure silicic acid uptake by marine phytoplankton, *Anal. Biogeochem.*, 78, 139–147, 1977a.
- Nelson, D. and Goering, J. J.: Near-surface silica dissolution in the upwelling region off north-west Africa, *Deep-Sea Res.*, 24, 65–73, 1977b.
- Nelson, D. and Smith, W.: Sverdrup revisited: critical depths, maximum chlorophyll levels, and the control of Southern Ocean productivity by the irradiance-mixing regime, *Limnol. Oceanogr.*, 36, 1650–1661, 1991.
- Nelson, D. and Tréguer P.: Role of silicon as a limiting nutrient to Antarctic diatoms: evidence from kinetic studies in the Ross Sea ice-edge zone, *Mar. Ecol.-Prog. Ser.*, 80, 255–264, 1992.
- Park, Y.-H., Charriaud, E., Ruiz Pino, D., and Jeandel, C.: Seasonal and interannual variability of the mixed layer properties and steric height at station KERFIX, southwest of Kerguelen, *J. Marine Syst.*, 17, 571–586, 1998.

Seasonal evolution of net and regenerated silica production

I. Closset et al.

Title Page

Abstract

Introduction

Conclusions

References

Tables

Figures

◀

▶

◀

▶

Back

Close

Full Screen / Esc

Printer-friendly Version

Interactive Discussion



- Park, Y.-H., Roquet, F., Durand, I., and Fuda, J.-L.: Large-scale circulation over and around the Northern Kerguelen Plateau, *Deep-Sea Res. II*, 55, 566–581, 2008.
- Park, Y.-H.: Water masses and circulation in the Polar Front region east of the Kerguelen Islands, *Biogeosciences Discuss.*, in preparation, 2014.
- 5 Pollard, R., Lucas, M., and Read, J.: Physical controls on biogeochemical zonation in the Southern Ocean, *Deep-Sea Res. II*, 49, 3289–3305, 2002.
- Pondaven, P., Fravallo, C., Ruiz-Pino, D., Tréguer P., Quéguiner B., and Jeandel, C.: Modelling the silica pump in the permanently open ocean zone of the Southern Ocean, *J. Marine Syst.*, 17, 587–619, 1998.
- 10 Pondaven, P., Ragueneau, O., Tréguer P., Hauvespre, A., Dézileau L., and Reyss, J. L.: Resolving the “opal paradox” in the Southern Ocean, *Nature*, 405, 168–172, 2000.
- Quéguiner, B.: Biogenic silica production in the Australian sector of the Subantarctic Zone of the Southern Ocean in late summer, 1998, *J. Geophys. Res.*, 106, 31627–31636, 2001.
- Quéguiner, B.: Iron fertilization and the structure of planktonic communities in high nutrient regions of the Southern Ocean, *Deep-Sea Res. II*, 90, 43–54, 2013.
- 15 Quéguiner, B. and Brzezinski, M.: Biogenic silica production rates and particulate organic matter distribution in the Atlantic sector of the Southern Ocean during austral spring 1992, *Deep-Sea Res. II*, 49, 1765–1786, 2002.
- Quéroué, F. et al.: Dissolved iron in the vicinity of the Kerguelen plateau (KEOPS-2 experiment), *Biogeosciences Discuss.*, in preparation, 2014.
- 20 Ragueneau, O., Treguer, P., Leynaert, A., Anderson, R. F., Brzezinski, M. A., DeMaster, D. J., Dugdale, R. C., Dymont, J., Fisher, G., François R., Heinze, C., Maier-Reimer, E., Martin-Jézéquel V., Nelson, D. M., and Quéguiner B.: A review of the Si cycle in the modern ocean: recent progress and missing gaps in the application of biogenic opal as a paleoproductivity proxy, *Glob. Planet. Change*, 26, 317–365, 2000.
- 25 Ragueneau, O., Savoye, N., Del Amo, Y., Cotten, J., Tardiveau, B., and Leynaert, A.: A new method for the measurement of biogenic silica in suspended matter of coastal waters: using Si: Al ratios to correct for the mineral interference, *Cont. Shelf. Res.*, 25, 697–710, 2005.
- Reynolds, B., Frank, M., and Halliday, A.: Silicon isotope fractionation during nutrient utilization in the North Pacific, *Earth Planet. Sc. Lett.*, 244, 431–443, 2006.
- 30 Roquet, F., Park, Y.-H. Guinet, C., Bailleul, F., and Charrassin, J.-B.: Observations of the Fawn Trough Current over the Kerguelen Plateau from instrumented elephant seals, *J. Marine Syst.*, 78, 377–393, 2009.

Seasonal evolution of net and regenerated silica production

I. Closset et al.

Title Page

Abstract

Introduction

Conclusions

References

Tables

Figures

◀

▶

◀

▶

Back

Close

Full Screen / Esc

Printer-friendly Version

Interactive Discussion



- Sarmiento, J., Gruber, N., Brzezinski, M., and Dunne, J.: High-latitude controls of thermocline nutrients and now latitude biological productivity, *Nature*, 427, 56–60, 2004.
- Sarthou, G., Chever, F., Qu  rou  , F., Bowie, A., Van der Merwe, P., Cheize, M., Sirois, M., and Bucciarelli, E.: Fe-Cu impact in incubation experiments of natural plankton communities and Fe- and Cu-binding ligand production at the vicinity of the Kerguelen Island, Southern Ocean, *Biogeosciences Discuss.*, in preparation, 2014.
- Strickland, J. and Parsons, T.: A practical handbook of sea water analysis, Fisheries research board of Canada, 167, 65–70, 1972.
- Tagliabue, A., Mtshali, T., Aumont, O., Bowie, A. R., Klunder, M. B., Roychoudhury, A. N., and Swart, S.: A global compilation of dissolved iron measurements: focus on distributions and processes in the Southern Ocean, *Biogeosciences*, 9, 2333–2349, doi:10.5194/bg-9-2333-2012, 2012.
- Takahashi, T., Sutherland, S., Wanninkhof, R., Sweeney, C., Feely, R., Chipman, D., Hales, B., Friederich, G., Chavez, F., Sabine, C., Watson, A., Bakker, E., Schuster, U., Metzl, N., Yoshikawa-Inoue, H., Ishii, M., Midorikawa, T., Nojiri, Y., K  rtzinger A., Steinhoff, T., Hoppema, M., Olafsson, J., Arnarson, T., Tilbrook, B., Johannessen, T., Olsen, A., Bellerby, R., Wong, C. S., Delille, B., Bates, N. R., and Debar H.: Climatological mean and decadal change in surface ocean $p\text{CO}_2$, and net sea–air CO_2 flux over the global oceans, *Deep-Sea Res. II*, 56, 554–577, 2009.
- Takeda, S.: Influence of iron availability on nutrient consumption ratio of diatoms in oceanic waters, *Nature*, 393, 774–777, 1998.
- Tr  guer P. and De La Rocha, C.: The World Ocean Silica Cycle, *Annual Review of Marine Science*, 5, 477–501, 2013.
- Trull, T., Rintoul, S., Hadfield, M., and Abraham, E.: Circulation and seasonal evolution of polar waters south of Australia: implications for iron fertilization of the Southern Ocean, *Deep-Sea Res. II*, 48, 2439–2466, 2001.
- Uitz, J., Claustre, H., Griffiths, B., Ras, J., Garcia, N., and Sandroni, V.: A phytoplankton class-specific primary production model applied to the Kerguelen Islands region (Southern Ocean), *Deep-Sea Res. I*, 56, 541–560, 2009.
- Zhou, M., Zhu, Y., d’Ovidio, F., Park, Y.-H., Durand, I., Kestenare, E., Sanial, V., Van-Beek, P., Qu  guiner B., Carlotti, F., and Blain, S.: Surface currents and upwelling in Kerguelen Plateau regions, *Biogeosciences Discuss.*, in press, 2014.

Seasonal evolution of net and regenerated silica production

I. Closset et al.

[Title Page](#)

[Abstract](#)

[Introduction](#)

[Conclusions](#)

[References](#)

[Tables](#)

[Figures](#)

◀

▶

◀

▶

[Back](#)

[Close](#)

[Full Screen / Esc](#)

[Printer-friendly Version](#)

[Interactive Discussion](#)



Table 1. Characteristics of the stations sampled for Si-fluxes measurements during KEOPS-2. Ze represents the bottom of the euphotic zone (1% of surface Photosynthetically Active Radiation), MLD is the depth of the Mixed Layer (from Park et al., 2014).

| Station | Zone | Position | | Date | Ze (m) | MLD (m) |
|---------|-------------|-------------|------------|--------|--------|---------|
| | | Latitude | Longitude | | | |
| R | HNLC | 50°21.55' S | 66°43.0' E | 26 Oct | 92 | 124 |
| E1 | Meander | 48°27.4' S | 72°11.3' E | 30 Oct | 64 | 69 |
| E3 | Meander | 48°42.1' S | 71°58.0' E | 4 Nov | 68 | 35 |
| F | Polar front | 48°31.2' S | 74°39.5' E | 7 Nov | 29 | 47 |
| E4W | Plume | 48°45.9' S | 71°25.5' E | 12 Nov | 31 | 55 |
| E4E | Meander | 48°42.9' S | 72°33.8' E | 14 Nov | 34 | 80 |
| A3 | Plateau | 50°37.5' S | 72°34.9' E | 17 Nov | 38 | 123 |
| E5 | Meander | 48°24.7' S | 71°54.0' E | 19 Nov | 54 | 41 |

Seasonal evolution of net and regenerated silica production

I. Closset et al.

Table 2. Biogenic silica concentration ($\int[\text{BSi}]$), Si-uptake ($\int\rho\text{Si}$), biogenic silica dissolution ($\int\rho\text{Diss}$), silica net production ($\int\rho\text{Net}$) and specific rates of Si-uptake and silica dissolution ($\int\text{VSi}$ and $\int\text{VDiss}$, respectively), integrated over the euphotic layer (1 % of surface Photosynthetically Active Radiation).

| Station | Zone | | | | | Specific rates | |
|---------|-------------|---|---|---|--|--------------------------------------|--|
| | | $\int[\text{BSi}]$ mmolm^{-2} | $\int\rho\text{Si}$ $\text{mmolm}^{-2}\text{d}^{-1}$ | $\int\rho\text{Diss}$ $\text{mmolm}^{-2}\text{d}^{-1}$ | $\int\rho\text{Net}$ $\text{mmolm}^{-2}\text{d}^{-1}$ | $\int\text{VSi}$ (d^{-1}) | $\int\text{VDiss}$ (d^{-1}) |
| R | HNLC | 33.28 ± 0.1 | 3.09 ± 0.01 | 4.88 ± 0.01 | -1.78 ± 0.02 | 0.09 | 0.15 |
| E1 | Meander | 96.1 ± 0.2 | 16.8 ± 0.1 | 7.11 ± 0.02 | 9.6 ± 0.1 | 0.17 | 0.07 |
| E3 | Meander | 83.6 ± 0.2 | 10.5 ± 0.1 | 9.99 ± 0.03 | 0.5 ± 0.1 | 0.13 | 0.12 |
| F | Polar front | 97.8 ± 0.5 | 27.5 ± 0.3 | 3.79 ± 0.03 | 23.8 ± 0.3 | 0.28 | 0.04 |
| E4W | Plume | 142.0 ± 0.7 | 31.8 ± 0.3 | 3.97 ± 0.03 | 27.9 ± 0.3 | 0.22 | 0.03 |
| E4E | Meander | 104.3 ± 0.5 | 21.0 ± 0.2 | $5.89 \pm 0.03^{\text{a}}$ | $15.1 \pm 0.2^{\text{a}}$ | 0.20 | 0.06^{a} |
| A3 | Plateau | 173.6 ± 0.7 | 47.9 ± 0.4 | 4.50 ± 0.03 | 43.4 ± 0.4 | 0.28 | 0.03 |
| E5 | Meander | 159.5 ± 0.4 | 27.5 ± 0.2 | 6.97 ± 0.03 | 20.5 ± 0.2 | 0.17 | 0.04 |

^a Since no dissolution rates were measured at E4E, these values do not correspond to calculations from direct measurements but only to estimations. Dissolution was calculated as the average of all KEOPS-2 integrated dissolution rates.

Title Page

Abstract

Introduction

Conclusions

References

Tables

Figures

◀

▶

◀

▶

Back

Close

Full Screen / Esc

Printer-friendly Version

Interactive Discussion



Seasonal evolution of net and regenerated silica production

I. Closset et al.

Title Page

Abstract

Introduction

Conclusions

References

Tables

Figures

◀

▶

◀

▶

Back

Close

Full Screen / Esc

Printer-friendly Version

Interactive Discussion

Table 3. Dissolution to production ratio ($\int D : \int P$), fraction of the silica production supported by new silicic acid ($1 - \int D : \int P$), and silicon to carbon (C) and nitrogen (N) uptake ratios (C and N assimilation were measured by Cavagna et al., 2014). ρN_{tot} represents both nitrate and ammonium uptake. All these values are integrated over the euphotic layer (1 % of surface Photosynthetically Active Radiation).

| Station | Zone | $\int D : \int P$ | $1 - \int D : \int P$ | gross- $\int \rho\text{Si} : \int \rho\text{C}$ | gross- $\int \rho\text{Si} : \int \rho\text{N}$ |
|---------|-------------|-------------------|-----------------------|---|---|
| R | HNLC | 1.58 | -0.58 | 0.28 | 0.44 |
| E1 | Meander | 0.42 | 0.58 | 0.38 | 1.27 |
| E3 | Meander | 0.95 | 0.05 | 0.18 | 0.74 |
| F | Polar front | 0.14 | 0.86 | 0.10 | 0.32 |
| E4W | Plume | 0.12 | 0.88 | 0.15 | 0.93 |
| E4E | Meander | 0.28 ^a | 0.72 ^a | 0.27 | 1.26 |
| A3 | Plateau | 0.09 | 0.91 | 0.30 | 1.51 |
| E5 | Meander | 0.25 | 0.75 | 0.35 | 1.41 |

^a Since no dissolution rates were measured at E4E, these values do not correspond to calculations from direct measurements but only to estimations. Dissolution was calculated as the average of all KEOPS-2 integrated dissolution rates.

Seasonal evolution of net and regenerated silica production

I. Closset et al.

Title Page

Abstract

Introduction

Conclusions

References

Tables

Figures

◀

▶

◀

▶

Back

Close

Full Screen / Esc

Printer-friendly Version

Interactive Discussion

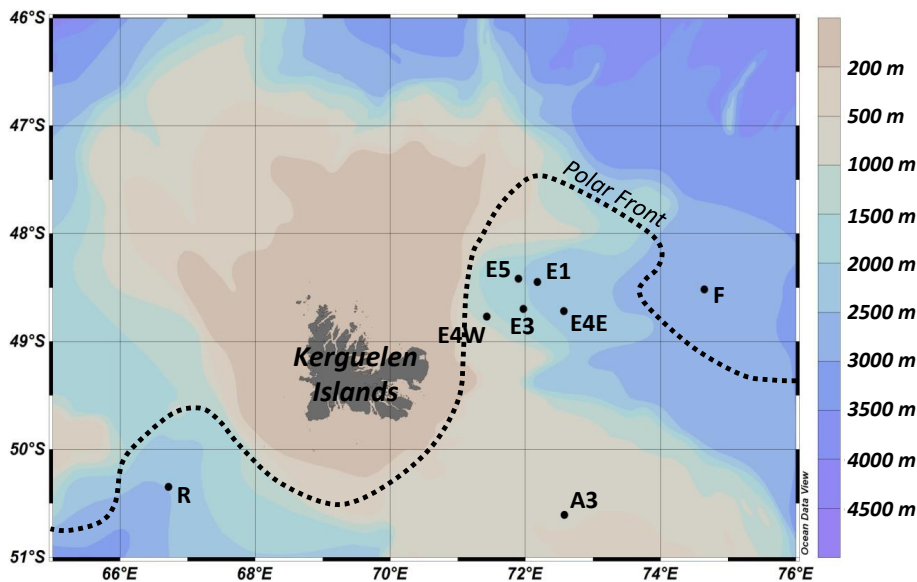


Fig. 1. Map of the KEOPS-2 cruise area (Indian sector of the Southern Ocean) showing the location of stations discussed in this study. Dotted line represents the position of the Polar Front from Park et al. (2014).

Seasonal evolution of net and regenerated silica production

I. Closset et al.

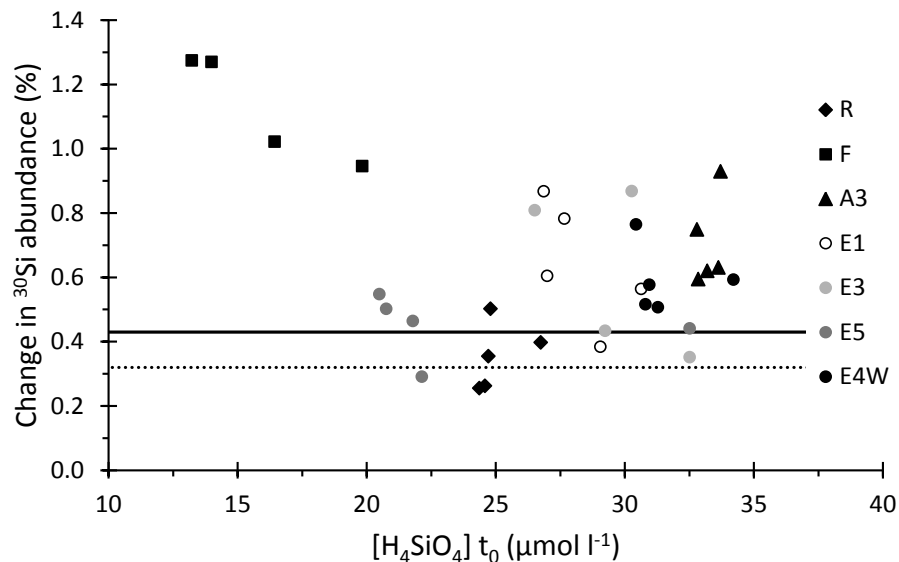


Fig. 2. Comparison of changes in ^{30}Si -abundance of seawater for each incubation (symbols) with detection limit of the ^{30}Si -isotopic dilution method (plain line) estimated from the reproducibility of an internal standard (0.43 %, $n = 40$). The dotted line represents the detection limit obtained from the average reproducibility of all dissolution duplicates (0.32 %, $n = 35$).

Title Page

Abstract

Introduction

Conclusions

References

Tables

Figures

◀

▶

◀

▶

Back

Close

Full Screen / Esc

Printer-friendly Version

Interactive Discussion



Seasonal evolution of net and regenerated silica production

I. Closset et al.

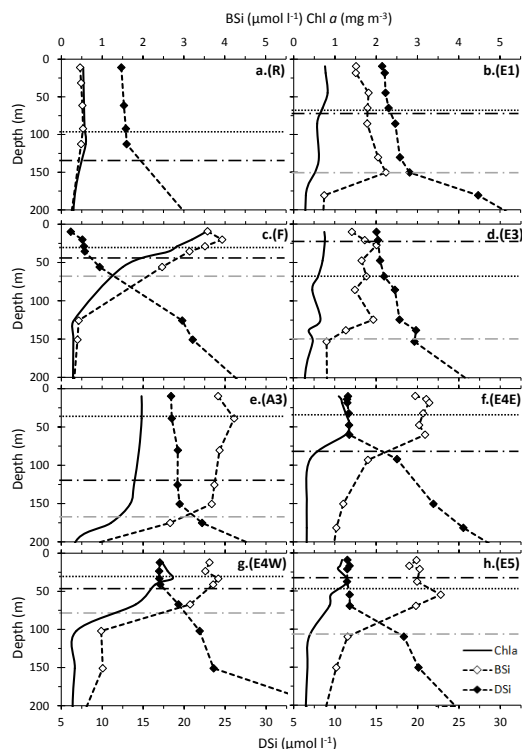


Fig. 3. Vertical distribution of chlorophyll *a* (continuous-black line; estimated from CTD fluorescence), biogenic silica concentration ([BSi], light dots) and H_4SiO_4 concentration ([DSi], dark dots). Dotted lines show the bottom of the euphotic layer (1 % of Photosynthetically Active Radiation, Z_e) for each station. Dark dashed lines represent the Mixed Layer Depth (MLD; estimated by Park et al., 2014) and grey dashed lines correspond to a 2nd density gradient identify from the density CTD-profile.

Title Page

Abstract

Introduction

Conclusions

References

Tables

Figures

◀

▶

◀

▶

Back

Close

Full Screen / Esc

Printer-friendly Version

Interactive Discussion



Seasonal evolution of net and regenerated silica production

I. Closset et al.

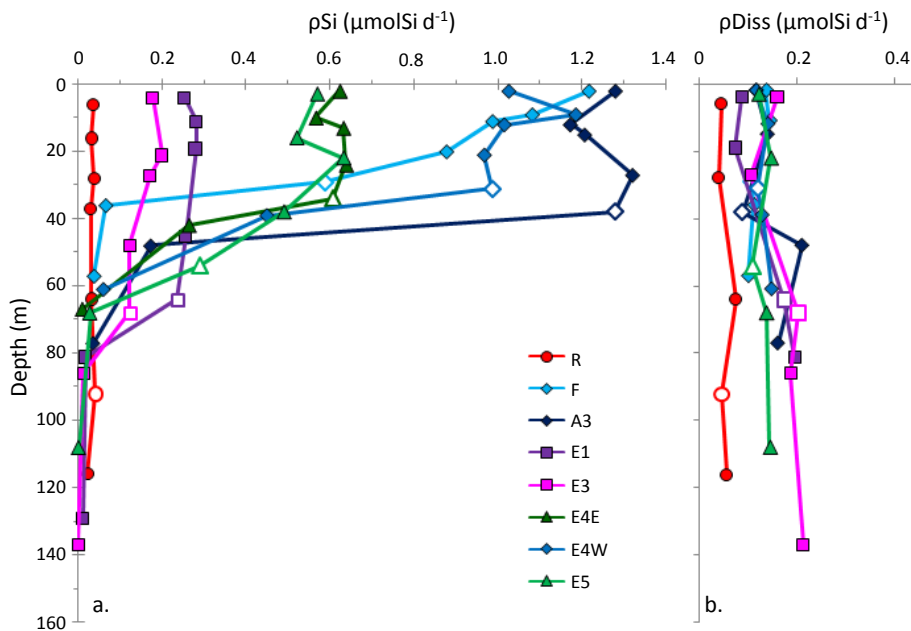


Fig. 4. Vertical distribution of Si-uptake (ρSi , panel **a**) and biogenic silica dissolution (ρDiss , panel **b**) in KEOPS-2 stations. Open symbols represent the depth at the bottom of the euphotic layer (1 % of Photosynthetically Active Radiation) for each station.

Title Page

Abstract

Introduction

Conclusions

References

Tables

Figures

◀

▶

◀

▶

Back

Close

Full Screen / Esc

Printer-friendly Version

Interactive Discussion



Seasonal evolution of net and regenerated silica production

I. Closet et al.

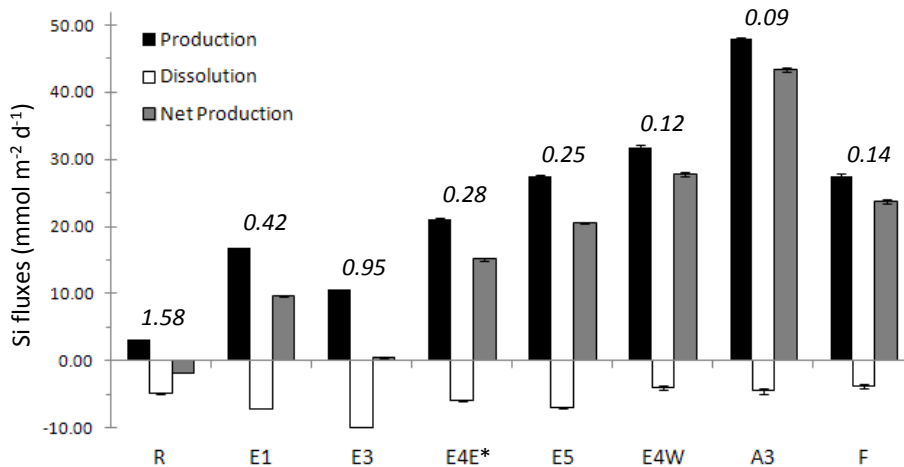


Fig. 5. Si-uptake (black), biogenic silica dissolution (white) and net silica production (grey) integrated over the euphotic layer (1% of Photosynthetically Active Radiation). Italic values correspond to the integrated dissolution to production ratio ($D:P$).

Title Page

Abstract

Introduction

Conclusions

References

Tables

Figures

◀

▶

◀

▶

Back

Close

Full Screen / Esc

Printer-friendly Version

Interactive Discussion



Seasonal evolution of net and regenerated silica production

I. Closet et al.

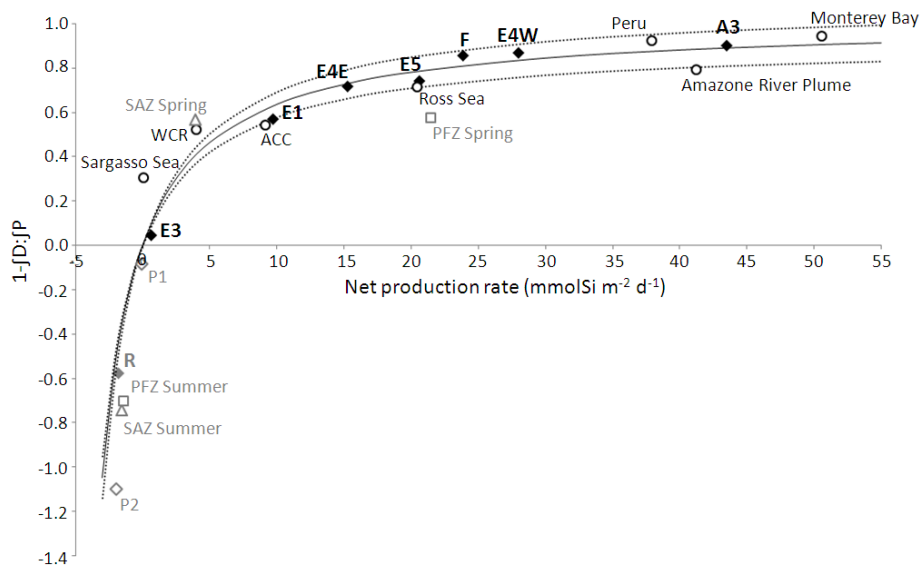


Fig. 6. Fraction of biogenic silica production supported by new silicic acid ($1 - \int D : \int P$) as a function of the integrated net silica production rate ($\int \rho_{\text{net}}$) during KEOPS-2 (filled black diamonds) compared with different regions of the global ocean (Open circles; Brzezinski et al., 2003 and references therein; and open diamonds; Fripiat et al., 2011b). Triangles and squares show the mean values for different growth seasons for SAZ and PFZ, respectively (Fripiat et al., 2011b). The plain line is a rectangular hyperbola to fit all data points (grey symbols were excluded from the model since they represent either negative $1 - \int D : \int P$ value which are not allowed by the model, or average while all other symbols refer to single stations). The equation of the curve is $1 - \int D : \int P = 1.01 \times \int \rho_{\text{net}} / (5.89 + \int \rho_{\text{net}})$. Dotted lines correspond to ± 1 sd of the $1 - \int D : \int P_{\text{max}}$.

Title Page

Abstract

Introduction

Conclusions

References

Tables

Figures

◀

▶

◀

▶

Back

Close

Full Screen / Esc

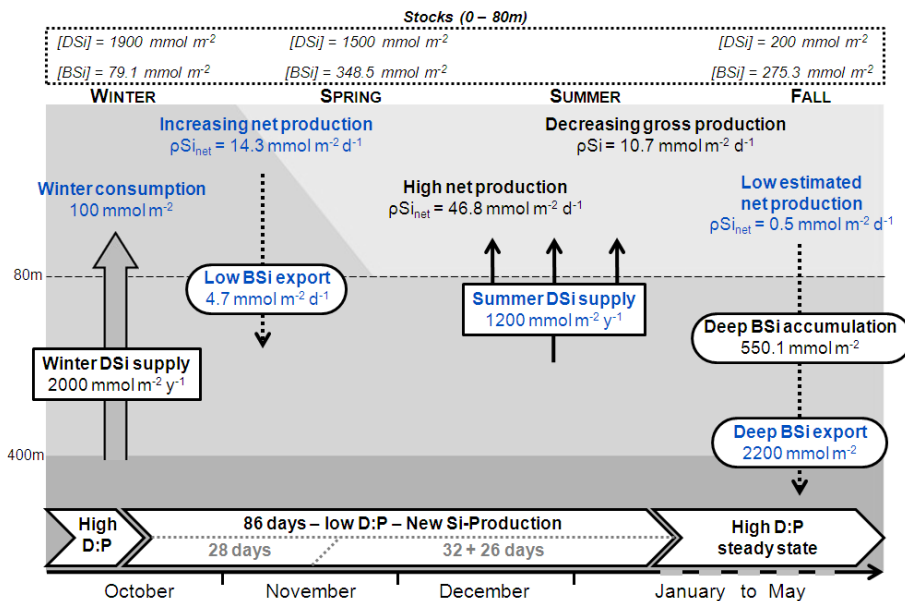
Printer-friendly Version

Interactive Discussion



Seasonal evolution of net and regenerated silica production

I. Closet et al.



Title Page

Abstract

Introduction

Conclusions

References

Tables

Figures



Back

Close

Full Screen / Esc

Printer-friendly Version

Interactive Discussion



Seasonal evolution of net and regenerated silica production

I. Closset et al.

[Title Page](#)

[Abstract](#)

[Introduction](#)

[Conclusions](#)

[References](#)

[Tables](#)

[Figures](#)



[Back](#)

[Close](#)

[Full Screen / Esc](#)

[Printer-friendly Version](#)

[Interactive Discussion](#)

Fig. 7. Schematic view of the seasonal silicon cycle in the mixed layer above the Kerguelen Plateau as estimated from natural and enriched Si isotopic measurements. Blue silicon fluxes correspond to estimated values while dark fluxes correspond to direct measurements. The 3 main water masses are represented by dark-grey for Upper Circumpolar Deep Water (UCDW), medium-grey for the Winter Water (WW) and light-grey for the Mixed Layer (ML). Variation of biogenic silica and H_4SiO_4 standing stocks integrated over 80 m (respectively [BSi] and [DSi]) are shown in the upper panel. Vertical continuous arrows represent DSi supplies from deep water to the ML, and dotted arrows correspond to particulate silica fluxes. Integrated silica production rates are calculated from the surface to 80 m. Horizontal white arrows represent the state of the bloom (indicated by the $D:P$ ratio) through time. Winter consumption has been estimated from the difference of winter mixing supply (Fripiat et al., 2011a) and the standing stock measured at the first A3 visit (KEOPS-2). The difference in standing stocks between the two visits at A3 (28 days, KEOPS-2) yields to the net silica production of $14.3 \text{ mmol m}^{-2} \text{ d}^{-1}$. The DSi standing stock at the second visit of A3 can sustain the net silica production measured for 32 days (this study) while the summer DSi supply estimated by Fripiat et al. (2011a) can sustain the same net production by an extra 26 days. The fall production measurements and standing stocks are from Mosseri et al. (2008, KEOPS-1). Since no silica dissolution is available from KEOPS-1, fall net production has been estimated from the difference between average gross silica production during KEOPS-1 (Mosseri et al., 2008) and average silica dissolution measured at all stations south of the Polar Front (KEOPS-2, this study). Deep BSi accumulation is calculated by integrating over the 100–200 m depth layer data from Mosseri et al., 2008 (see text for further details).